UNIVERSITAT POLITÈCNICA DE VALÈNCIA

ESCUELA TÉCNICA SUPERIOR INGENIERÍA INDUSTRIAL VALENCIA

BIOMEDICAL ENGINEERING MASTER THESIS

DEVELOPMENT OF A ROBUST P-WAVE DELINEATION METHOD FOR ELECTROCARDIOGRAPHIC RECORDINGS BASED ON GAUSSIAN MODELING. EVALUATION ON STANDARD AND CUSTOMIZED DATABASES

AUTHOR: Francisco González Molina

SUPERVISOR: José Joaquín Rieta Ibáñez

SUPERVISOR: Raúl Alcaraz Martínez

Academic year: 2019-20

Dedicado a mis tutores, José Joaquín y Raúl.

Por su confianza en los inicios e inestimable guía durante todo el camino.

Por su comprensión e infinita paciencia.

Gracias.

Abstract

Atrial Fibrillation is the most common sustained cardiac arrhythmia. Its prevalence is even expected to increase in the coming years. Indeed, it is already considered an epidemic disease. However, the degenerative physiological mechanisms guiding its development are currently not fully understood. Therefore, still a more research effort in this field is needed. Along this line, the study of surface cardiac signals has been presented as an easily accessible source of useful information about the heart's condition. Particularly, the state of the atria can be characterized through the study of the P-wave in the electrocardiogram, which represents its electrical activity. For this, in this Master's dissertation an automatic P-wave delineation method has been developed. The novel strategy applied for delineating P-waves regardless their morphology is based on the creation of a Gaussian model of each waveform and the use of morphological information of preceding P-waves to guide the fiducial points location. For validation purposes the manual annotations of the standard QT database from Physionet were used. The results provided a detection sensitivity of a 100%, whereas the mean and standard deviation of the error committed with respect to the reference set by the database were for the P-wave onset, P-wave peak and P-wave offset, 4.71 ± 9.59 ms, 2.82 ± 6.69 ms and 0.6 ± 9.79 ms, respectively. The results obtained, which outperform others presented in the literature, exhibit that the proposed method is a reliable, accurate and robust delineator. Therefore, this algorithm might be presented as a valuable tool for identifying the gradual modification in the electrophysiological properties of the atria that has been highly associated with the occurrence and maintenance of cardiac pathologies such as Atrial Fibrillation.

Contents

Chapter 1

Introduction

1.1 Motivation

Atrial fibrillation (AF) is the most common sustained arrhythmia in the clinical practice, affecting around 2% of the population worldwide [1]. Furthermore, in the following years, the prevalence of AF is expected to increase due to the improvements achiveved in its diagnosis, in the the treatment of related cardiac and noncardiac diseases, as well as the ageing demographics [1, 2]. AF is described as a rapid and irregular activation of the atria, leading to a defective function [3]. Despite not being a direct lethal condition, it may lead to blood clots formation, stroke, myocardial infarction or heart failure among other cardiac complications, resulting in an increased mortality [4].

Ongoing research on AF supports that several degenerative mechanisms, such as electrical, structural and autonomic remodeling, are involved in the initiation and maintenance of AF [3]. However, the physiopathology of AF is currently not fully understood [5]. Therefore, much more research is still needed in order to improve our understanding about the mechanisms underlying this arrhythmia, allowing an earlier diagnosis and more effective treatment [6].

Whithin this context, the analysis of cardiac signals has received great interest [7]. In particular, the study of the surface electrocardiographic (ECG) signal of patients suffering from atrial fibrillation has been presented as a highly valuable tool for the non-invasive assessment of the heart's condition [8]. Commonly, the ECG signal has been used for AF diagnosis. However, its usefulnes is spreading to new applications such as the success evaluation of specific therapies or the assesment of the degree of atrial remodeling [9].

In the ECG, the P-wave is the waveform associated with the atrial activity. So, abnormalities in the atrial conduction pattern will be reflected in this waveform morphology [10]. During AF, the ECG is characterized by the substitution of the normal P-wave for rapid and irregular oscillations called f-waves [11]. The focus of analysis in this work has been centered in the P-wave morphology during sinus rythm, prior the onset of an AF episode [8].

Disorders in the electrical properties of the atria are widely associated with the maintenance of AF, such as intra and interatrial conduction delays and heterogeneous electrical conduction due to the possibly presence of fibrosis [9]. This phenomena can be reflected in several P-wave morphology indices such as its duration and dispersion, which is the difference between the widest and the narrowest P-wave [12]. As a result, in recent years, the analysis of the P-wave has become a major focus of attention for the study of atrial tachycardias, and specially AF [9, 13].

The averaged-signal P-wave has been usually analyzed to minimize the effect of its low SNR levels, caused by its reduced amplitude [14]. Hence, prolonged P-waves duration and P-waves dispersion have been associated with a higher risk of AF compared with healthy controls [15, 16] or after cardiac surgery [17, 18], and a greater probability of transition from paroxysmal to permanent AF [19]. Not only long but also short P-waves duration have been associated with higher risk of AF [20]. In addition, morphological changes as notched or deflected P-waves together with longer duration, have been proven to be a strong indicator for the development of AF [21]. Finally, the morphology variability, calculated by correlating the P-waves with a template [22], or using the standard deviation of the euclidean distance between them [23], has been also revealed as indicator of AF presence.

Plenty of useful information can be extrated from the averaged-signal P-wave analysis. However, averaging does not allow the analysis of the individual waveforms and their variability over time. This possibility migth be interesting because of the progressive nature in which the electroanatomical properties of the atria are modified leading to the initiation of AF [22]. Thereby, the identification of changing P-wave morphology patterns during sinus rhythm indicating a remodeling process in the atria may allow the prediction of an AF episode before it actually occurs [24, 25]. This phenomenon is relevant because the success rate achieved by the strategies currently followed to maintain sinus rhythm such as anthyarrythmic drugs or ablation techniques is significantly lower for more advanced AF [26]. Furthermore, catheter ablation higher success rate reduces the need for redo procedures and hospitalization time, which represents the major cost driver in AF care. Consequently, this improvement in the AF management could reduce significantly the cost burden on the healthcare system [27].

The primary steps to obtain useful infomation from P-waves are their individual detection and delineation along the ECG signal. However, the lack of consensus among physicians about the precise location of P-wave fiducial points hinders this delineation process [28]. Furthermore, this task is highly time-demanding and requires significant levels of concentration, which makes it tedious and tiring [29]. Having this in mind, the main motivation of this work is the development of an automatic method capable of accurately detect and delineate P-waves in the ECG regardless of their morphology, thus reducing the inherent subjectivity of manual annotations.

1.2 Hypothesis and Main Goal

In recent years, considerable research effort has been directed towards the development of methods capable of delineating P-waves in the ECG. Numerous P-wave delineators have been developed based on different mathematical principles [30]. In general, the strategy underlying all these methods consist of enhancing somehow the waveform pattern of the P-waves to facilitate their delineation. However, this approach might modify the original morphology, thus compromising the resulted fiducial points allocation. Thereby, the hypothesis of the present work is that the use of a model of each individual P-wave to guide its delineation process will allow a more accurate delineation, as it preserves the original P-waves morphology pattern. In addition, the use of morphological information from already delineated waveforms might improve the robutness of the delineation algorithm.

Therefore, this Master's Dissertation is aimed at developing a novel robust algorithm capable of accurately delineating any kind of P-wave using Gaussian models and hitorical morphological data. A previous delineation of a gaussian function modeling each P-wave would delimit the region of the waveform in which the fiducial points are searched. Also, historical morphological information is taking into account for the delineation , thus improving the accuracy and robustness of the method.

The peformance of this algorithm was compared with other other methods presented in the literature by taking the manual annotations of a standard ECG database as reference. The strategy followed migth reduce the delineation error, providing a common and reliable framework that will enhance the development of diagnosis tools to identify diverse atria phenomena. Consequenly, it might enable the development of more personalized and effective treatments and, ultimately, might contribute to the health improvement of people affected by adverse cardiac conditions, such as AF.

1.3 Structure of this document

This document is structured in the following chapters:

- **Chapter 2: General Background.** This chapter reviews some relevant concepts aimed at establishing the proper theoretical framework of this Master's Disertation.
- **Chapter 3: Gaussian guided P-wave delineation method.** The novel P-wave delineation method proposed in this work is described in detail in this chapter.
- **Chapter 4: Validation Database: QTDB.** The characteristics of the standard database used for the proposed method validation are presented.
- **Chapter 5: Results and Discussion** The evaluation procedure of the method is described and the consequent results obtained are shown together with other comparable algorithms. Also, Several aspects are discussed in this section, such as the assessment of the results obtained and the main strengths and limitations of the method.
- **Chapter 6: Contributions and Future Work.** The concluding remarks are exposed, as well as the main scientific contributions derived from this work and future lines of research.
- **Chapter 7: Budget.** The costs associated with the development of this Master Dissertation.

Chapter 2

General Background

2.1 Anatomy and Physiology of the Heart

The human heart is a muscle about the size of a fist. It is located in the chest, between the lungs and above the diaphragm. The heart is in charge of pumping blood through the circulatory system to the lungs, in order to produce the exchange of gases and, to the whole body, to supply oxygen and nutrients to the tissues and remove wastes, such as carbon dioxide [31]. In this section, the main structures of the heart are described and it is explained how it performs electrophysiologically.

2.1.1 Anatomy of the Heart

The heart can be seen as two pumps operating in series, with the pulmonary and systemic circulations in between [32]. The pulmonary circulation corresponds to the flow of blood within the lungs that allows the exchange of gases between the blood and alveoli. The systemic circulation is formed by all blood vessels within and outside the rest of organs in the body, to provide them oxygen and nutrients and remove carbon dioxide and other wastes [33]. The right atrium receives venous blood, which is deoxygenated and at low pressures, from the systemic circulation through the superior and inferior vena cava. After that, the blood moves passively to the right ventricle. The right ventricle then contracts, pumping the blood into the pulmonary system by way of the pulmonary artery. Next, the oxygenated blood coming from the lungs enters the left atrium through the pulmonary veins and then flows to the left ventricle. Finally, this chamber ejects the blood into the aorta by means of its contraction distributing it at high pressure to the rest of the body tissues [32, 33].

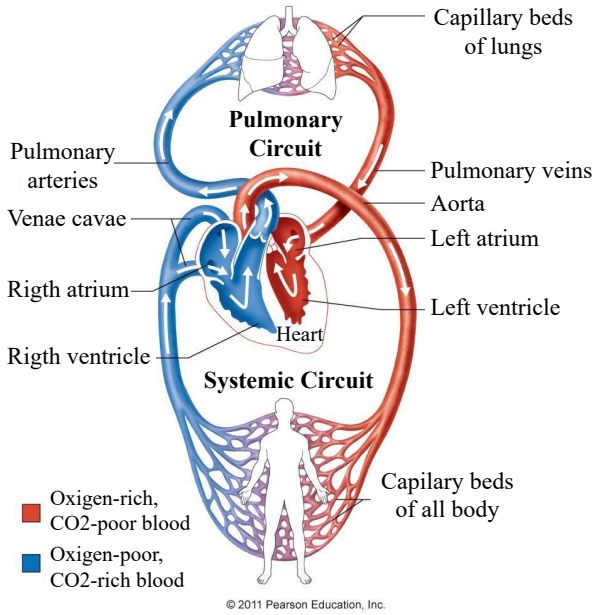

Figure 2.1: Scheme representing the cardiovascular system. Arranged in series, the rigth and left side of the heart with the pulmonary and systemic circulation between them. Blue: deoxygenated blood; Red: oxygenated blood. Also main vessels and chambers are labelled [34].

In Figure 2.2, a closer look to the heart structures is shown. The walls of the heart are composed of cardiac muscle or *myocardium*. The right atrium is a highly distensible chamber, which allows its expansion to accommodate the low pressure venous return. On the other hand, the left ventricle has a thick muscular wall, as high pressure is needed to be produced during its contraction to eject blood into the systemic arterial system, which is in charge of the distribution of blood at high pressures to the whole body [33]. Between each atrium and its respective ventricle, there is a valve that prevent blood from flowing backwards. The names of the atrioventricular (AV) valves are tricuspid and mitral, for the right and left side of the heart, respectively. The papillary muscles are attached to fibrous strands of these valves and to the ventricular wall. These connections prevent AV valves from bulging back and leak blood into the atria [33]. In addition, two more valves can be found in the heart: the semilunar valves. These structures, pulmonary and aortic valves, receive that name for their crescent-shaped cups. They separate each ventricle with their corresponding great arteries [32]. Finally, the cardiac wall that separates both ventricular chambers is called the interventricular septum [33].

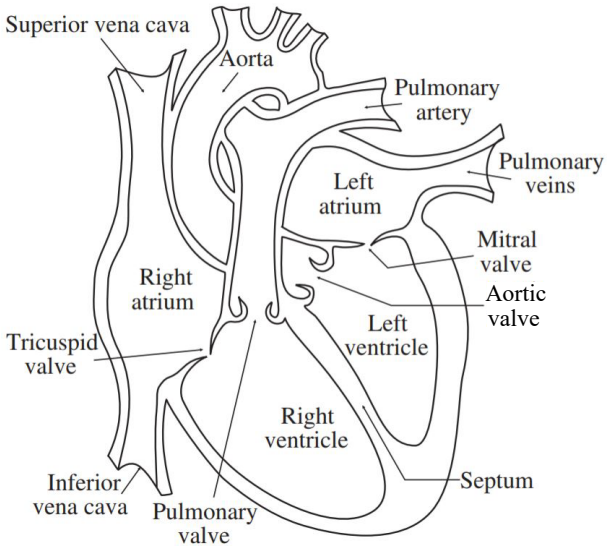

Figure 2.2: Structure of the anatomy of the human heart and associated vessels [35].

2.1.2 Physiology of the Heart

The physiology of the heart may refer to several aspects such as the blood flow or pressure. However, this work will be centered on the electrical activity of the heart that stimulates the cardiac cells producing the periodic movement of the muscle. The mechanical activity of the heart is rhythmically produced following an ordered sequence of chambers contractions. This mechanism is driven by the electrical stimulation of different cardiac cells areas, allowing an efficient pumping of the blood [32].

The heartbeat is initiated and controlled by certain groups of myocardial cells that are able to spontaneously generate electrical impulses that are propagated through the cardiac tissue. This capacity is called automaticity. Normally, the activation starts in the sinoatrial (SA) node, which is located between the superior vena cava and the right atrium. This region, due to its higher firing rate, acts as the cardiac pacemaker. The depolarization wave initiated in the SA node propagates, first, to the right atrium, and then, to the left atrium. After that, the conduction velocity is reduced when passing through the atrioventricular (AV) node, which gives time to the ventricles to be filled. Next, the depolarizing wave enters the bundle of His, which is a rapidly conducting structure made up of Purkinje cells that bifurcates into rigth and left branches (RBB and LBB). These structures reach the ventricular myocardium rapidly, thus producing a synchronized ventricular activation [7, 32]. All the aforementioned structures within the heart are shown in Figure 2.3.

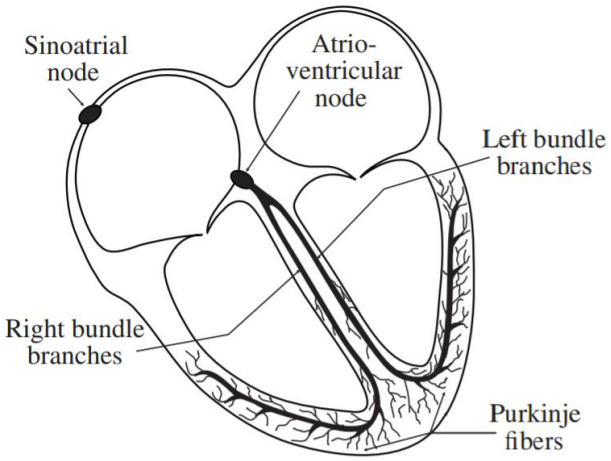

Figure 2.3: Representation of the main structures involved in the electrical conduction system of the heart [35].

2.2 The Electrocardiogram

The electrocardiogram is the non-invasive representation of the heart's electrical activity. When cardiac cells depolarize and repolarize, an electrical current spreads through the tissue. These voltage variations, caused by the action potentials of the cardiac cells that lead to the contraction of the myocardium, can be measured by surface electrodes [7]. The recorded ECG represents the differences in potential captured by electrodes to observe the morphology and timing of the heart's electrical activation, providing information about the initiation of the electrical impulses, the pathway of the cardiac muscle depolarization as well as the conduction velocity and rythm [7, 32, 33].

Einthoven, in the late 19th century, invented the string galvanometer that measured for the first time the electrical activity of the heart [36]. He also named the deflections observed as P, Q, R, S and T [32]. These names are mantained still nowadays. In Figure 2.4 a segment of an ECG trace is shown and one of the repeated waveforms patterns is expanded and labelled showing all relevant waves, intervals and segments. The P-wave is the first deflection recorded by the ECG and it is caused by the atrial depolarization. The period of time between the onsets of the P-wave and QRS complex is called P-R interval and represents the time between the initiations of atrial and ventricular depolarizations, associated with the time that it takes the expulsion of the remaining blood for the atria into the ventricles during the AV nodal delay. The QRS complex represents the rapid ventricular depolarization and the T-wave its repolarization. The isoelectric ST segment is the period between the end of the QRS complex and the beginning of the T-wave, corresponding with the plateau phase of the

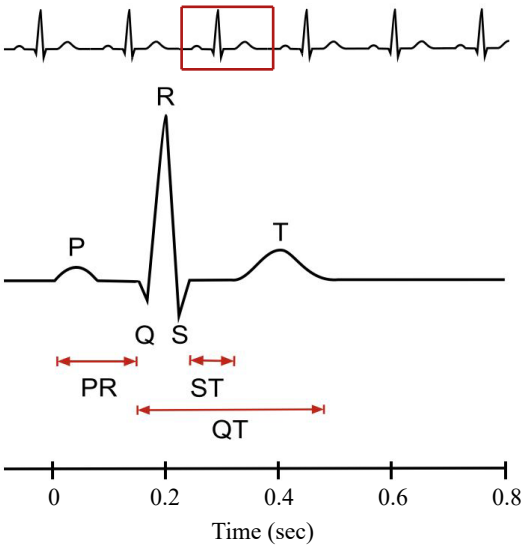

Figure 2.4: Typical electrocardiogram recording (top). Bellow it, one of the repeated waveforms patterns enlarged with all deflections and relevant time periods labelled [33].

ventricular action potential. Finally, the QT interval represents the duration of the ventricular action potential and it extends from the QRS onset to the T-wave offset [32, 33].

The wave of depolarization and repolarization can be represented as an electrical vector. Thus, the magnitude and direction of this vector with respect to the recording electrode will determine the polarity and amplitude of the corresponding waveform in the ECG [33]. Using different electrodes we can obtain information about the cardiac vector from different angles. These views of the electrical activity of the heart are called leads. When the depolarization spreads towards a lead it causes an upward deflection while when it spreads away from the lead, a downward one [37]. Therefore, the number and location of the surface electrodes are significant for the ECG interpretation as they can give us complete information about the sequence of activation of the different parts of the heart. The standard configuration is called the 12-lead system. It requires 10 electrodes whose positioning is summarized in Figure 2.5. In this configuration there are three types of ECG leads: Bipolar standard limb leads, unipolar augmented limb leads and unipolar chest leads. For the monopolar leads, a virtual electrode called *Wilson Central Terminal* or *WCT* is produced by averaging the measurements from the RA, LA and LL electrodes [33]. How the 12 leads are obtained is shown in Table 2.1.

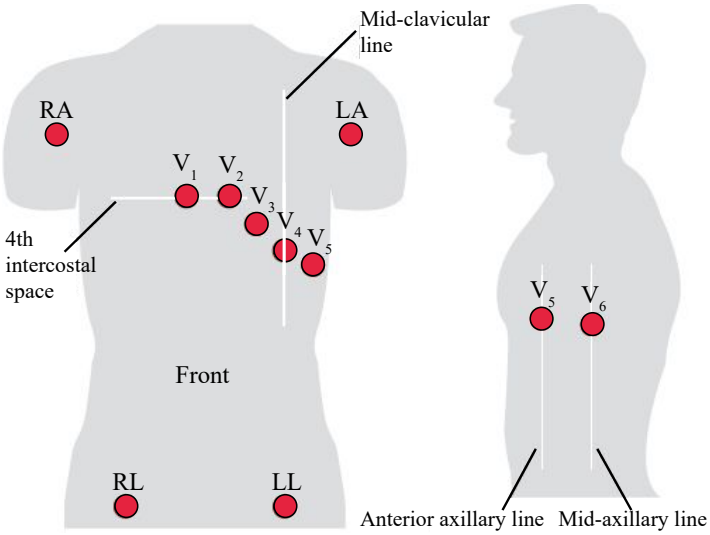

Figure 2.5: Electrodes placement for the 12 leads ECG [38].

Type	Lead	Calculation
Standard limb leads	I	LA-RA
	II	LL-RA
	III	LL-LA
Augmented limb leads	aVR	-(I+II)/2
	aVL	I - (II/2)
	aVF	II - (I/2)
Precordial leads	V1	V1-*WCT*
	V2	V2-*WCT*
	V3	V3-*WCT*
	V4	V4-*WCT*
	V5	V5-*WCT*
	V6	V6-*WCT*

Table 2.1: Name and type of the leads of the standard 12-leads system and how they are calculated.

2.3 Atrial Fibrillation

As commented in previous sections, the primary pacemaker of the heart is the SA node. Its discharge rate in resting conditions ranges from 60 to 100 times per minute, which defines a normal heart rate [32]. However, under certain circumstances, the heart beats taking other rhythm different from the considered normal, this is called arrhythmia. When the heart rate is slower than usual is named bradycardia and when it is sustained at rates greater than 100 beats per minute, tachycardia. Also, arrythmias are classified based on the structure involved, the atria or the ventricles [32].

Atrial Fibrillation is the most common sustained arrhythmia. The American College of cardiology (ACC), American Heart Association (AHA) and European Society of Cardiology (ESC) defined AF as a supraventricular tachyarrythmia characterized by uncoordinated atrial activation that provoke the deterioration of the atrial mechanical function [5]. In 2010 it has been estimated that 20.9 million women and 12.6 million men will be affected by this arrhythmia [5]. However, the prevalence of AF is believed to be underestimated. Sometimes, this arrhythmia occurs in the absence of symptoms and, consequently, it is difficult to be detected [1]. Therefore, several factors such an improved AF detection, aging society and favorable environmental conditions for this arrhythmia, lead the developed world to a situation in which one in four middle-age adult will suffer from AF [5].

AF can be classified based on the presentation, duration and spontaneous termination of the episodes. Traditionally, five types of AF can be considered: First diagnosed AF, when it has not been diagnosed before; Paroxysmal AF, when is self-terminating within seven days; Persistent AF, when the episode lasts more than a week and requires medical intervention to be terminated; Long-standing persistent AF, when continous AF under a rhythm control strategy lasts for more than a year and Permanent AF, when the patient and physician decide not to intervene to control the rhythm [5].

The pathophysiological mechanisms of initiation, maintenance and termination of AF are not completely understood [39]. For the initiation of AF are needed both a trigger and substrate [40]. The triggers are foci that prematurely activates. These groups of cells with abnormal automaticity are commonly located in some specific atrial structures. The most frequent source of triggers are the pulmonary veins [41]. The substrate for AF initiation and maintenance is mainly cardiac tissue with electrical heterogeneity in terms of different refractory periods. This condition is favored by the phenomena of the atrial electrical and structural remodeling [40].

Atrial remodeling stands for any persistent alteration of the atrial structure or function [42]. This concept, introduced by Wijffels and coworkers in the mid nineties, has remarkably broaden our understanding of AF pathophysiology [43]. They discovered that continuous rapid atrial pacing in the goat heart model resulted into progressive shortening of the atrial effective refractory period (AERP) and increased duration of AF. This direct relationship identified between pacing duration and AF maintenance, led them to enunciate the statament "AF begets AF", which perfectly defines the progressiveness of this process [43].

Atrial remodeling during AF and its progressive nature is explained by two major mechanisms, electrical and structural remodeling [44]. Electrical remodeling of the atria happens in terms of AERP shortening or rate adaptation loss. Also, this process has been proven to be reversible within a few days [43]. On the other hand, structural remodeling is more permanent. It is characterized by the anatomical alteration of cardiomyocites, originating dilated and fibrotic tissues that migth serve as potential substrate for AF maintenance [45, 46].

Several disorders such as heart failure, hypertension, cardiovascular diseases, diabetes, valvular and ischemic heart disease, among others, may promote these changes in the atria. In addition, as it was stated before, AF itself can contribute to provoke this atrial remodeling that facilitates the maintenance of this arrhythmia, worsening its prospect of termination [40].

In general, it is accepted that the mechanism mantaining AF can be a rapid focal ectopic firing or a reentrant wavelet that can be single and localized or multiple varying in time and space [47, 48]. However, several other hypothesis have been proposed, such as the doubled layer hypothesis, multiple wavelet mechanism, rotors, transmural reentry circuits, etc [40]. In conclusion, there is a controversy about the main mechanisms responsible of AF and, therefore, still much more research is needed to fully understand the physiopathology of this arrhythmia.

2.4 P-wave delineation methods

In previous sections of this work it has been already highlighed the great applicability of P-wave morphological information in a clinical context. However, the absence of standardized measurement techniques and quality control assessments represents a major limitation for their adoption as a source of daily clinical information for decision making [28]. Also, it has been exposed the inconveniences of manual determination of P-wave morphological characteristics and the resulting need for the development of authomatic P-wave delineation methods. However, this is not a simple task, due mainly to the lack of consensus for the precise location of the initial and final points of this waveform. Consequently, considerable research effort has been directed towards the development of methods capable of delineating P-waves, either individually or together with other waves within the ECG. Thus, in recent years many different P-wave delineators have been introduced based on various principles.

Many delineation methods have explored the use of diverse kind of mathematical transforms. This approach consists in changing the P-waves pattern to ease its delineation. For instance, the discrete Fourier transform has been applied [49], as well as the discrete cosine transform [50] or the phasor transform [51]. However, the wavelet transform is currently the most extended strategy for P-wave delineation. This option operates in a similar way to a filterbank, thus reducing the frequency content of the signal, which simplifies the waveform pattern and helps its delineation. The use of the wavelet transform for this purpose was initially proposed in 1995 by Li et al. [52], study that years later inspired the method presented by Martínez et al. [53]. Other researchers have adopted this approach for their delineation methods due to the significant noise effect reduction that can be achieved and the low signal-to-noise ratio that characterize the P-wave [29, 54–56].

Other strategies have been also employed, such as the use of matching templates which correlates each P-wave signal with known patterns [57], dynamic time warping [58, 59] or probabilistic and statistical methods, such as hidden Markov models [60, 61] or Bayesian techniques [62]. Additionaly, the very first relevant method presented for P-wave delineation was based on the differentiation of the ECG signal. The peaks were identified as zero crossing points and the P-wave onset and offset were calculated based on a search of points exceeding certain thresholds calculated empirically in function of the maximum slope of the waveform [63]. The derivative searching approach has been also explored in [64]. In this case an adaptive threshold was adopted, taking into account the slope and high frequency noise of the signal. In [65] a methodology based on an adaptive threshold, as well

as an adaptive size of search windows for P and T-wave detection, has been proposed.

It should be noted that the novel method presented in this work takes inspiration from this last strategy, adding new features that will be described in depth in the next chapter.

Chapter 3

Gaussian guided P-wave delineation method

The delineation process of the method presented in this Master's dissertation is in this chapter described. First, it will be shown the signal conditioning used and, later, a detailed explanation of the delineation algorithm itself.

3.1 Preprocessing of the ECG recording

The ECG signal is affected by many external agents that may alter its authentic morphology: muscle noise, power line interference, electrode contact noise, baseline drift, motion artifacts, etc [8]. Therefore, it is needed the application of a preliminary step of preprocessing to reduce the influence of this noise in the signal.

In this initial step the cardiac signal is first resampled up to 1 kHz, if it was not already. This sampling frequency is considered a "de facto" standard and has been widely recommended for ECG analysis [8]. Then, the baseline wander is removed from the raw ECG signal through subtracting the signal envelope [7], and the 60 Hz frequency component corresponding to the powerline interference is canceled through an adaptive filtering which preserves the spectral content of the ECG signal [66]. After that, high frequency muscle noise content is reduced by using a method based on the wavelet transform. This kind of filtering have been reported as more respectful with the pattern morphology of cardiac signals, decreasing the level of noise in the signal [67, 68]. Finally, remaining high frequency

noise is additionally reduced by applying an 8th order bidirectional Chebyshev low-pass filter with a 70 Hz cut-off frequency [69].

Other published methods [29, 59, 63] present a much more aggressive filtering of the ECG signal. Probably, this choice is motivated by the usual consideration that the normal P-wave spectral range is strictly limited to low frequencies (10-15 Hz) [7]. However, it has been demonstrated the existence of much higher frequency components in the P-wave [7]. This evidence, along with the corresponding reduction of the transient effects aggravated by the proximity of the QRS complex, motivated the decision of using a less aggressive filtering.

As a last step of the signal preprocessing, every QRS complex along the ECG recording is located to have a temporal reference point for the detection of each P-wave on it. For this purpose, R-peaks are initially detected using two different methods, one of them based on the wavelet transform and another based on signal derivatives [70]. Results were supervised in order to have a trustworthy R-peaks detection. It should be noticed that the purpose of this work is the development of a reliable method for P-wave delineation. Therefore, all this effort oriented to the R-peaks proper location, even if probably excessive, was dedicated to avoid a final result biased by an error in these peaks detection.

3.2 The proposed algorithm for P-wave delineation

In a normal sinus rhythm ECG recording, it has been assumed certain degree of repetitiveness in the temporal location and morphology of the P-waves along the signal. Accordingly, in the proposed method, a record of certain parameters calculated from previously delineated waveforms, is kept. This information will be used to guide the detection and delineation of following waves. Two of these parameters are the temporal location of the search window (SW) in which the P-waves are sought, with respect to the R-peak position, and its length. Also, some morphological parameters are taken into account, such as the differences in time and amplitude between the P-wave maximum peak and its boundaries, and the morphology. To this last respect, four types have been considered: Monophasic Positive ($+$), Monophasic Negative ($-$), Biphasic ($positive - negative$) and Biphasic ($negative - positive$). These adaptive parameters are employed both to make potential decisions during the delineation process and to detect possible anomalies in a particular wave morphology. Naturally, these adaptive parameters have to be initialized. This process will be accomplished in a preliminary phase of initialization in which a reference P-wave is constructed such as described in the next subsection.

3.2.1 Obtaining the reference P-wave

At this early stage of the delineation process, the signal segments prior to each of the first five R-peaks detected in the preprocessing step are averaged to create a representative excerpt, such as shown in Figure 3.1. Thus, the initial values of the aforementioned parameters are obtained from this reference signal excerpt (RSE).

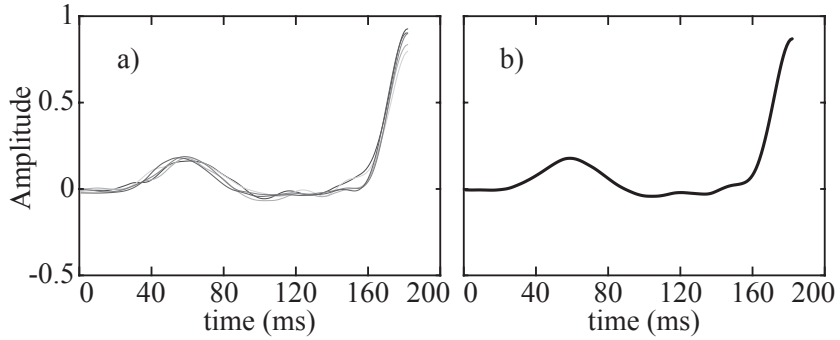

Figure 3.1: Representation of five ECG excerpts prior their respective R peaks overlapped (a) and their average: RSE (b).

The position of the QRS onset in RSE is first estimated. This location has been defined as the point preceding the R-peak for which the signal slope exceeds a 15% of the maximum slope value for more than 20 milliseconds. This condition is established as the existence of a resting time between the P-wave ending point and the QRS onset, in which the signal slope should be significantly smaller, is known. This outcome is not intended to be the precise location of the QRS onset, but an estimation of its situation as a safeguard against a potential misclassification of the Q-peak.

Then, the peak of the representative P-wave that is taken as reference is searched. A possible linear trend in RSE is initially subtracted and then, this peak is sought in a search window extended from the previously approximated QRS onset position. The searched window length was defined here as one third of the RR distances median value [65]. The search process is carried out by simply locating the peak of greater amplitude. This naive approach of detecting P-waves has been recently compared with other strategies, such as line fitting or wavelet transform, resulting to be more successful [71]. After that, a piece of signal is isolated around the detected peak, corresponding to the reference P-wave (RPW). Its length was determined as 200 ms, a 33% more of which is considered the width of a normal P wave (120 ms) on each side. Even though, if the median RR interval value is too long (>900 ms) or too short (<600 ms), the length of RPW is increased or reduced by 20 ms, respectively. In

addition, this interval is restricted to the right by the estimated position of the QRS onset previously calculated plus a resting time of 15 ms. In Figure 3.2 it can be observed two examples of RSE, the detection of the maximum amplitude peak position (a) and around it, the P-wave isolated (b). This overdone value was chosen to assure a width larger than any possible P-wave morphology [29]. In addition, the P-wave maximum peak is not always centered, and particularly not in the case of biphasic waveforms.

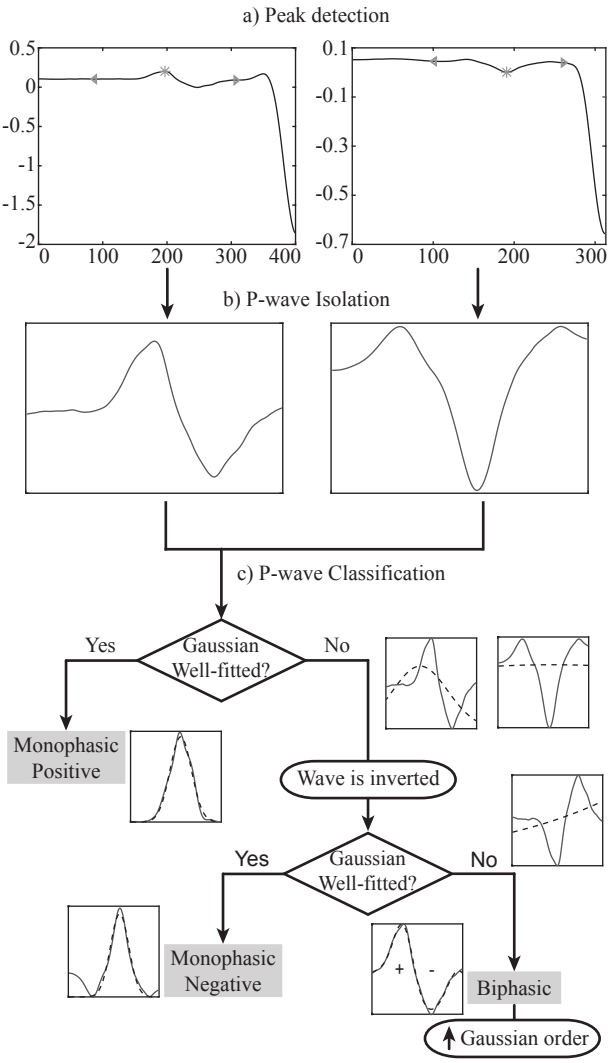

Figure 3.2: Sequential description of the classification process of a P-wave, illustrated with by examples: a) RPW peak and boundaries detection among the RSE, b) isolation of the RPW and c) decision tree for the P-wave classification itself, with a graphic example of each possible situation.

Once RPW is isolated, the morphological classification process is performed through a decision tree as illustrated in Figure 3.2. Initially, a first order Gaussian function is generated so that it fits the

RPW in the best way possible, maximazing the R-squared value. Later, it is evaluated if the fitting is sufficiently good for P-wave delineation. For this method, the correlation value used to decide if the fit is good enough or not was heuristically determined to be 0.7. In case the Gaussian function fits the RPW properly, it is classified as Monophasic Positive. Otherwise, this procedure is repeated from the beginning with the RPW inverted. The new fit is again assessed and, depending on the success or not, is classified, respectively, as Monophasic Negative or Biphasic. For the latter case, in which RPW is labeled as biphasic, it is searched a second peak with reverse polarity than the one previously found. After that, the RPW is recalculated by centering the middle position between both peaks. After that a Gaussian model of the waveform is created, increasing the order of the Gaussian function. Initially, a second order Gaussian function is created. However, it was observed that for some cases this was not enough to get a proper model. Therefore, in these cases, the use of up to a fourth order Gaussian function was considered.

3.2.2 Delineation of the reference P-Wave

After the RPW morphology classification, its boundaries are sought. For the delineation process, the Gaussian function that resulted well fitted to the signal in the preceding step, is first delineated. However, one characteristic of the Gaussian functions that may differ from a P-wave is its symmetry. Thus, for an asymmetric P-wave, it will not be possible to obtain a suitable Gaussian model in any case. Hence, before the delineation is started, a final evaluation of the goodness of fit again through R-squared value is made in both halves of the waveform. This procedure is shown in Figure 3.3 by means of an example. Thus, if one of the halves is poorly adapted to the model (or both, as in the case presented in Figure 3.3) an artificial wave is created by meeting this particular half of wave with itself mirrored. Later, another Gaussian model of the artificial wave is created and half of it is used for the delineation. In the case presented in Figure 3.3, it can be observed an improvement in the goodness of fit after this procedure has been performed. To evaluate the fitting goodness it was used the same approach explained before.

Then, to carry out the P-wave delineation, the Gaussian model is first differentiated. For each half of the differentiated waveform, the maximum value is next identified. These are the points in which the Gaussian function presents their maximum slopes. Later, based on these values, a slope threshold is calculated. From maximum slope point location to the left or right, depending if the onset or offset

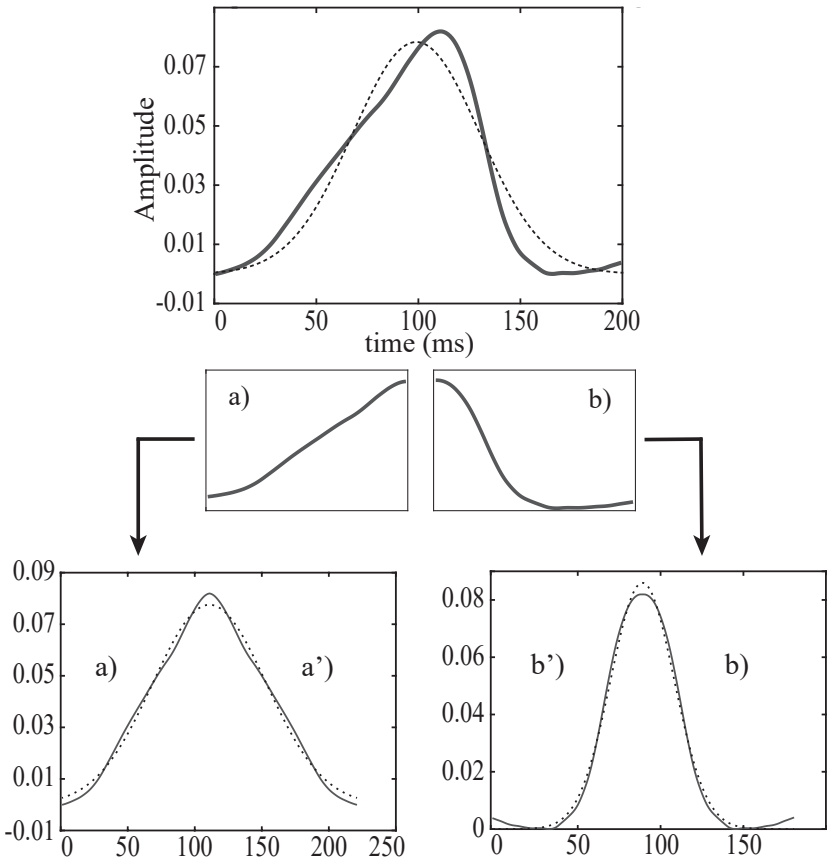

Figure 3.3: Representation of a P-wave (solid line) and its Gaussian model (dotted Line) bad fitted because of its asymmetry and the creation of two artificial waveforms by meeting each half of it, a) and b), with their respective mirrored versions, a') and b'), to obtain better Gaussian fits in both cases.

of the wave is being searched, respectively, the first slope value to exceed the slope threshold is labeled as the fiducial point sought [63].

To determine the function that defines the threshold in each case, it is necessary to know the relationship between the maximum slope of a waveform and the slope value in the position where the corresponding fiducial point is located. To find this relation the boundaries from 60 P-waves were manually annotated by two expert physicians. The slope values of each waveform in these points were obtained and plotted against their corresponding maximum slopes, thus resulting in the graph shown in Figure 3.4. Then, the best fit, minimizing the least squares sum, was sought by testing different kind of functions such as linear, logarithmic, exponential, etc. Finally, the rational function presented in equation (3.1) and shown in Figure 3.4, resulted to be the best fit, with an R-square score of 0.815. The function obtained mathematically defines the slope threshold.

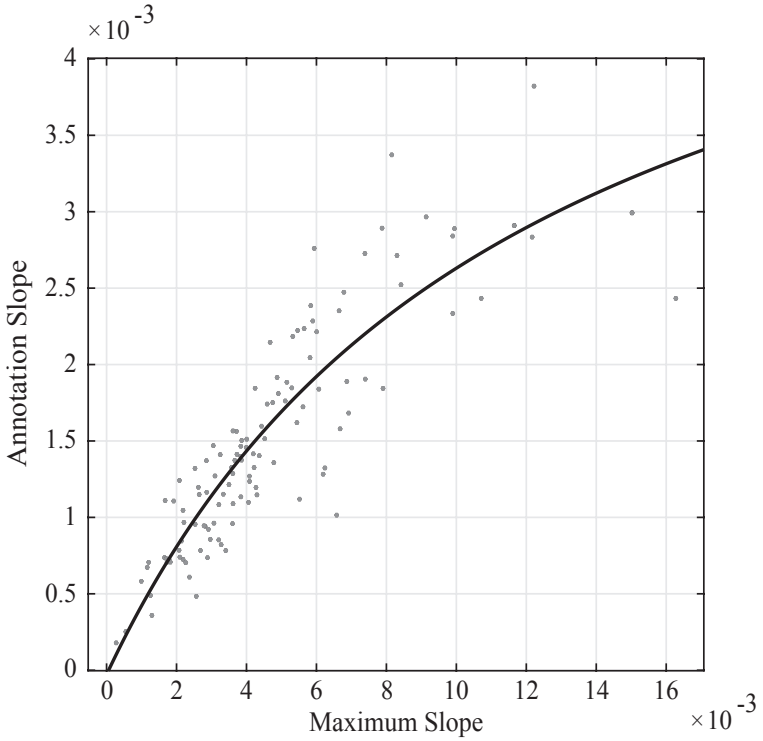

Figure 3.4: Relationship between the slope values in the annotated points (onset and offset) and their respective maximum slopes in 60 different P-waves. The black solid line shows the best possible fit determined by equation (3.1).

$$f(x) = \frac{0.0058x}{x + 0.012} \tag{3.1}$$

After the Gaussian model has been delineated, the same delineation process is repeated with the real P-wave. However, in this case the area in which fiducial points are searched is restricted to the vicinity of its counterparts in the Gaussian model. These restricted intervals centered on the onset and offset positions of the Gaussian function are indicated as shaded areas in Figure 3.5. The width of these regions around each fiducial point depends on the goodness of the Gaussian fit. Thus, Figure 3.5 shows how this interval is greater in the left half of the waveform as its Gaussian fits worsens. Specificaly, the width was determined depending on the Pearson correlation coefficient as shows Table 3.1.

Finally, when the boundaries of the RPW have been determined, they will be used to define the length of the search window for the coming delineation.

From representative P-wave already delineated, information is also obtained as reference to ease the delineation of every individual P-wave. More preciesly, differences in time and amplitude between

Pearson correlation coefficient (PCC)	Search window width
PCC $\geq$ 0.995	10 ms
0.995 $>$ PCC $\geq$ 0.993	16 ms
0.993 $>$ PCC $\geq$ 0.99	20 ms
0.99 $>$ PCC $\geq$ 0.95	40 ms
PCC $<$ 0.95	50 ms

Table 3.1: Searching window width with respect to the Pearson correlation coefficient.

the maximum peak of the waveform and its boundaries, the approximated position of the wave with respect to the R peak, the width of the search window, the waveform morphology and some starting coefficients for the Gaussian fit.

3.2.3 Individualized P-wave delineation

With all the information obtained from the previously exposed initialization step, all P-waves are individually detected in the already defined search window (SW) prior to their corresponding R-peaks. Initially, the P-wave peak is detected and checked if it is centered on the SW. So, if the waveform peak is not located in the central 30% of the SW, its position is readjusted by sliding it to center the peak location within the SW.

The delineation method is mostly the same as the applied before to the RPW, but with just slight differences that are detailed below. The main drawback in this case is the possible existence of more than one candidate for fiducial point. This may occur because the morphology of the P-waves found could be more complex than the one created during the initialization stage. Thus, there could be found multiple points meeting the requirements to be considered onset or offset of the waveform. This is shown in Figure 3.6, where a P-wave with three offset candidates is presented. The final decision is based on the aforementioned morphology parameters. Thus, in Figure 3.6 option c) would be first discarded as it is not within the restricted interval for fiducial points searching. Finally, between the two remaining options, a) would be selected as it is closer to the point determined by the morphology parameters calculated based on previously delineated waveforms.

Moreover, after each P-wave is delineated, previously mentioned parameters are recalculated taking into account the new information obtained from this new waveform. Specifically, new parameters have an influence ratio of a 20% over the existing ones. This weight was chosen to be consequent with the five waveforms taken for the initialization stage. Before updating each parameter, the difference

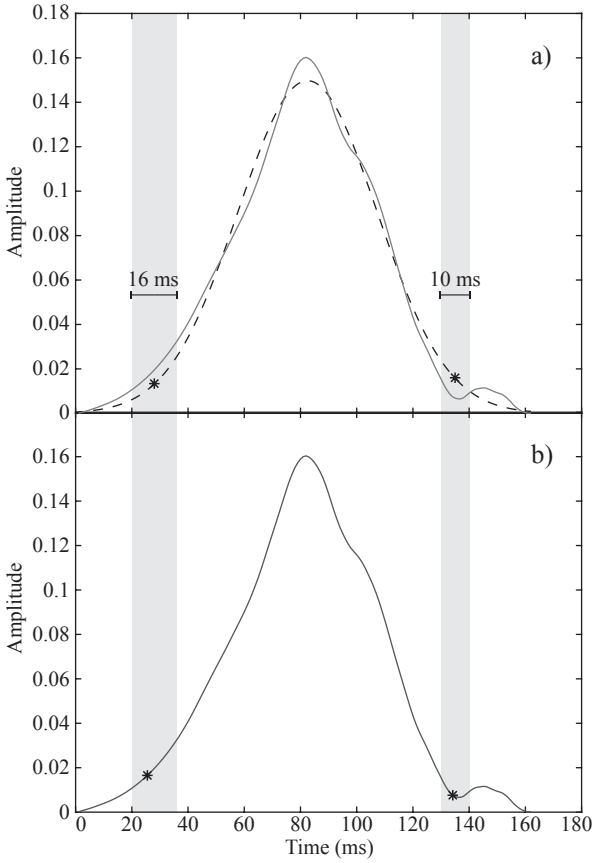

Figure 3.5: The onset and offset positions of the Gaussian wave are marked with asterisks and also, around them, a gray area representing the time interval in which the fiducial points can be sought in the real signal. In the bottom, the same P-wave is represented with their fiducial points positions highlighted the gray region.

with respect to the current value is checked. In case the variation is greater than 25%, the wave is labeled as abnormal and the parameter is not updated.

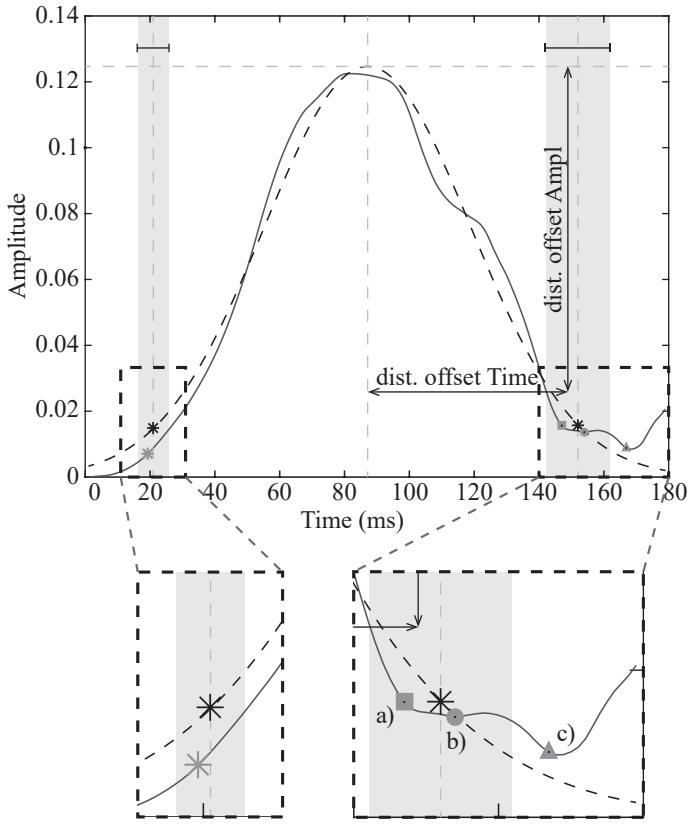

Figure 3.6: An example of a P-wave (solid line) and its model Gaussian function (dotted line) in which, on the right side, there are shown with gray asterisks three candidates to be the offset of the waveform represented by different figures. Also the boundaries of the Gaussian waveform (black asterisks) and a representation of the parameters used for the candidates selection (distance in time and amplitude between the peak and the offset calculated by taking into account previous waveform morphologies) are shown.

Chapter 4

Validation Database: QTDB

To evaluate the performance of an algorithm, an enviroment for testing as realistic as possible is required. More specifically, a wide variety of signals from the real world, before being implemented in a clinical context, are needed [7].

The availability of public and freely accesible databases for this process might enable the development of reliable algorithms, as well as fair comparisons among all developed methods. Since there are several databases to validate the fiducial points delineation in the ECG, first, the characteristics of all of them are reviewed. After that, the one selected for this study is described in detail.

4.1 Available databases for validation of P-wave delineators

For this work we have reviewed the characteristics of the most relevant ECG databases:

- **MIT-BIH arrhythmia database** [72]: It was the first compilation of standard ECG recordings available for the public domain. It was created by the Arrhythmia Laboratory of Beth Israel Hospital in Boston in the 1970's to allow the evaluation of arrhythmia detectors and the comparison between the different algorithms. The database contains 48 two-channel holter ECG excerpts of 30 minutes each selected specifically to include anomalous but clinically relevant arrhythmias. Initially, only the QRS complexes were automatically annotated with the later supervision and correction of expert cardiologists who also labelled abnormal beats and categorized the rhythm and signals quality. However, in 2015 Elgendi et al. provided P and T wave peak manual annotation for one of the channels of the MIT-BIH Arrhythmia Database [73].

- **AHA database**: This long-term ECG database was created at the Washington University in St. Louis by a group headed by G. Charles Oliver for the evaluation of Ventricular Arrhythmia detectors during the late 1970's and early 1980's. It contains 80 two-channel holter recordings of 35 minutes each. The recordings are annotated beat-by-beat. However, this database is not freely available.

- **European ST-T database** [74]: This database was born in response to the growing interest in the analysis of ST-T meassurements as indicative of myocardial ischemia. It was designed at the CNR Institute for Clinical Physiology in Pisa and contains 90 two-hour excerpts of two-channel long-term ECG recordings. The leads recorded were placed on non necessarily standard locations in the chest, where it was considered most likely ST-T changes to be revealed. Cardiologists added annotations of the QRS complexes and beat types, episodes of change in ST segment or T wave morphology and their onset, peak and offset. Also changes in the rhythm and signal quality were labelled.

- **CSE multilead measurement database** (CSEDB) [75]: This database includes 250 recordings of 10 seconds each with the 12 standard leads and the Frank's leads X, Y and Z data. It also provides annotations for the onset and offset of the P, QRS and T wave. The annotations were obtained by five referee cardiologists and 11 different programs. However, the experts just analyzed some of the samples of the multilead library and those in which the results of different programs were far from the median value, resulting that just a few number of beats (32) were manually annotated. In addition this database is not public.

- **Chinese Cardiovascular Disease Database** (CCDD) [76]: This standard 12 leads ECG database contains up to 1250 annotated recordings. The annotations, including onset and offset of P-QRS-T vawes, morphology features and beat diagnosis, were made by two expert physicians. This database is freely available.

4.2 The QT database

Despite all the options described above, in this work, the standard database selected for validation purposes was the **QT Database** (QTDB), which is freely available at Physionet [77]. The QT Database [77] has been adopted by the scientific community as the reference database for the validation of

numerous delineation algorithms due to the wide variety of QRS, T and P wave morphologies that it contains and, because there is hardly any freely available alternative that presents a great number of boundary annotations made manually by experts physicians. More specifically, the vast majority of P-wave delineation methods published has taken this database as reference for validation purposes. This is due to the wide variety of P-wave morphologies that it presents, with manual annotations of the onset, offset and peak of more than 3000 different waveforms from recordings specifically selected to reflect the real world variability [77]. The QTDB contains 105 fifteen-minutes two leads ECG recordings sampled at 250 Hz. It was designed to help to evaluate the performance of automatic ECG waveforms duration measurement methods, and especially the QT interval [77]. The origin of these recordings are other existing databases such as the MIT-BIH Arrhythmia Database, the European ST-T Database and other ECG databases collected at Bostons's Beth Israel Hospital [77]. It also contains manual annotations made by expert physicians in at least 30 beats per recording, determining the timing of different fiducial points of the P, QRS, T and U waves. The beats annotated were specifically selected to represent the dominant morphology of the signal and the annotation procedure was performed at full scope. For this strategy, a common location for each fiducial point in all leads presented, is determined.

In the QTDB two sets of annotations can be found. Each one of these was provided by a different cardiologist. However, only one of them has been used in this work as it contains a considerably greater number of annotated waveforms. In Figure 4.1 two consecutive manually annotated P-waves from the QTDB are shown. Specifically, both channels of the 19^{th} and 20^{th} annotated beats from the recording called *sel117* are displayed.

4.2.1 Analysis of the quality of the QTDB manual annotations

To decide the precise location of P-wave boundaries there is no clear and unique criterion in the scientific community. Therefore, since there is no gold standard, it is difficult to determine whether an annotation is sufficiently accurate or not. However, the error in the location of the onset and offset of a waveform is perfectly obvious in some cases. In Figure 4.1 it can be easily appreciated how the P-wave offset of the second beat is far from the intuitive area in which the end of the waveform should be located. Note that the defective annotation is apreciated in both channels. This is relevant as no information was provided about which one was used for the manual annotation process.

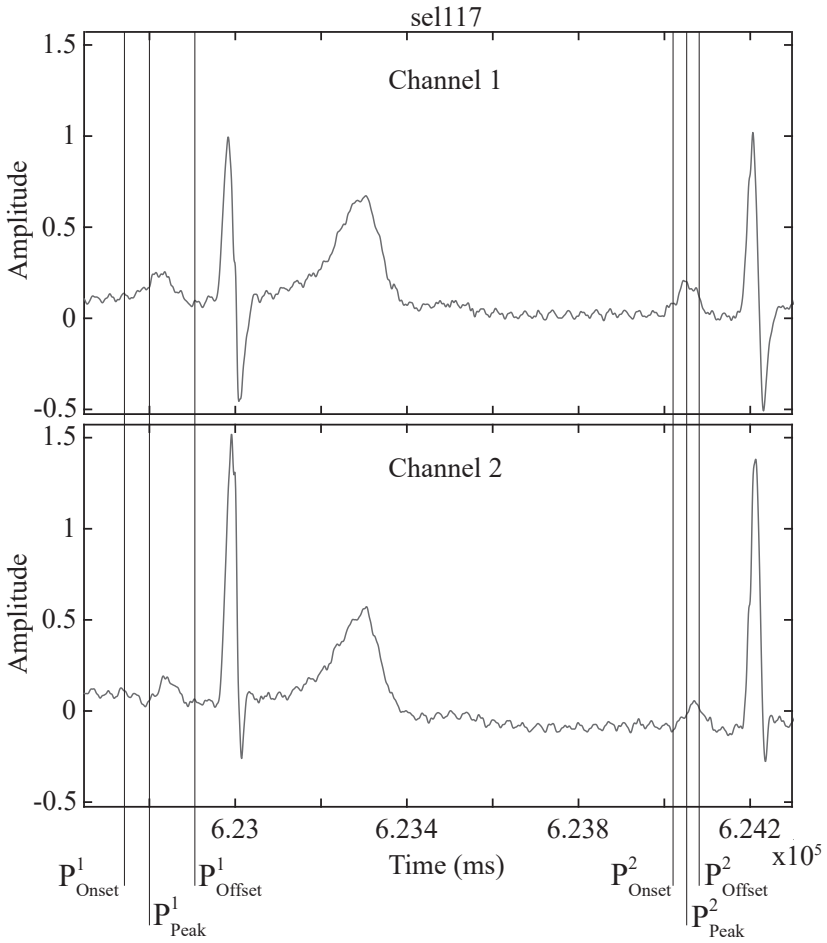

Figure 4.1: Two consecutive P-waves manually annotated from the QTDB.

Apart from the annotation criteria, signal noise can also affect the quality of the annotation. In Figure 4.2 two annotated P-waves from different recordings are shown prior and after reducing the noise level on them. Specificaly, the 30^{th} annotated beat form *sel230* recording and the 5^{th} annotated beat from *sele0211* recording. It can be observed how the P-waves boundaries accuracy is reduced when the noise level in the signal is reduced. Note that the QTDB recordings manual delineation was performed whithout applying any denoising algorithm.

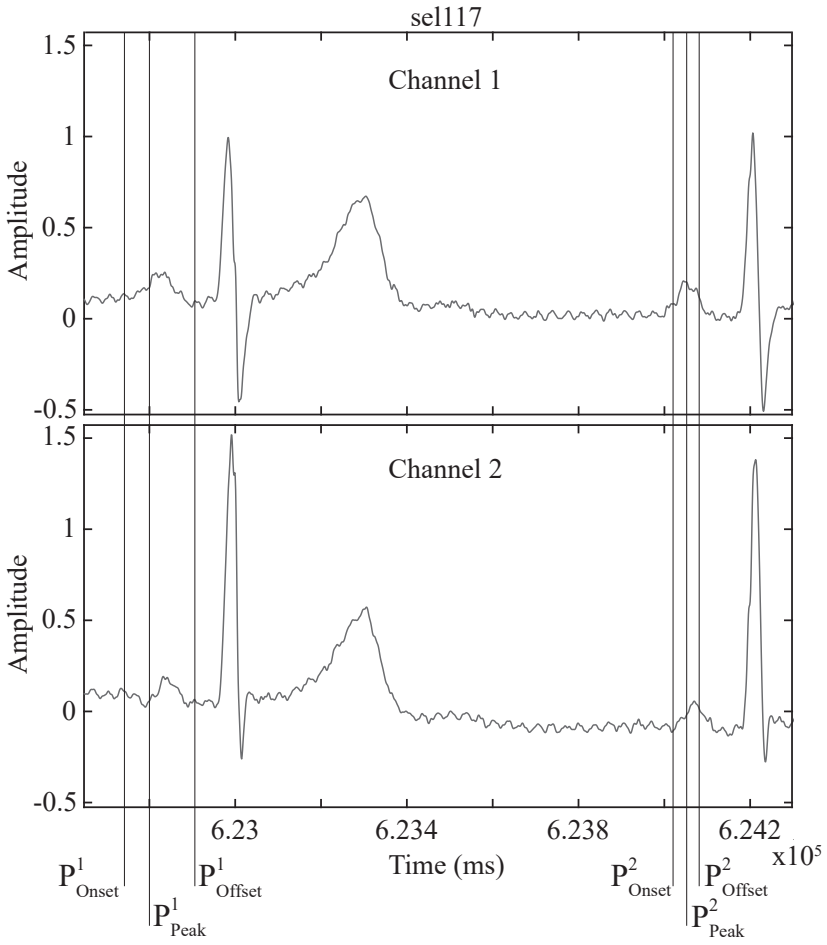

Figure 4.2: Two P-waves manually annotated from the QTDB prior and after filtering the noise content in the signal.

Chapter 5

Results and Discussion

5.1 Results

5.1.1 Assessment of P-wave delineation

The detection performance of the proposed method has been evaluated by means of the Sensitivity (Se). This parameter indicates the percentage of events properly detected. The mathematical definition of this statistical measurement is described as:

$$Se = \frac{TP}{(TP+FN)} \tag{5.1}$$

where TP refers to true positives detections and FN to false negative detections.

To determine a missed detection a temporal window centered within the reference point should be defined. Some studies such as [78] or [61] have used a window length of 150 ms, value in accordance with the ANSI/AAMI-EC57:1998 standard [79]. Others have adopted a less demanding value such as 170 ms [80] or 320 ms [81] and many others do not specify this information [53, 63]. For this work a more strict value of 80 ms has been selected.

The error committed for each automatic annotation is calculated as the time difference with respect to the Cardiologists' one. Thus, to asses the proposed delineation algorithm, a global score is determined in terms of the average value of the error (μ) and its standard deviation (σ) measured in milliseconds (ms), such as in previous works.

5.1.2 Results for P-wave delineation

In Table 5.1 are shown the proposed method results. For comparison, the results reported from other relevant studies that have presented their delineation results for all fiducial points considered in this work, using more than 3000 beats from the QTDB, are shown. In addition, in the last row it has been included the acceptable σ error for each fiducial point with respect to manual annotations defined by the CSE Working Party [82]. This group stablished a set of recomendations with the objective of standarizing electrocardiographic measurements. Among them, a set of values of acceptable tolerance limits for the standard deviation of the annotation diferences from the reference for several ECG fiducial points, were listed.

Specifically, for P-wave onset and offset, standard acceptable σ error tolerances of 10.2 and 12.7 ms, were provided respectively. Actually, different tolerances values depending on the specific lead used for the delineation process were defined. However, in this case the average value was selected as no information was provided about the specific lead used for each QTDB recording.

Methods	Validation Parameters	P_{ON}	P_{PEAK}	P_{OFF}
This method	Se(%)	**100**	**100**	**100**
	$\mu \pm \sigma$(ms)	**4.7±9.6**	**2.8±6.7**	**0.6±9.8**
Martínez	Se(%)	98.65	98.65	98.65
et al. [51]	$\mu \pm \sigma$(ms)	2.6±14.5	32±25.7	0.7±14.7
Martínez	Se(%)	98.87	98.87	98.87
et al. [53]	$\mu \pm \sigma$(ms)	2.0±14.8	3.6±13.2	1.9±12.8
Laguna	Se(%)	97.7	97.7	97.7
et al. [63]	$\mu \pm \sigma$(ms)	14±13.3	4.8±10.6	−0.1±12.3
Rincon et al. [83]	Se((%)	99.87	99.87	99.91
	$\mu \pm \sigma$(ms)	8.60±11.20	10.10±8.90	0.90±10.10
Lin et al. [62]	Se((%)	89.93	98.93	98.93
	$\mu \pm \sigma$(ms)	3.70±17.30	4.10±8.60	-3.10±15.10
CSE Working group [82]	2σ(ms)	10.2	-	12.7

Table 5.1: Comparison of the delineation performance of some of the most relevant P-wave delineation methods in the literature by means of three Validation Parameters making use of the QTDB.

The results of this method exposed above were obtained using a total of 3176 beats from 96 of the 2-leads ECG recordings from the QTDB. From the original set of 105 recordings, 7 of them (*sel102*, *sel221*, *sel232*, *sel310*, *sel36*, *sel37*, *sel50*) were excluded as no P-wave manual annotation was provided. Also recordings *sel104* and *sel36* were not delineated as they did not present a minimum of three consecutive annotated P-waves.

Additionally, the method was applied to the original set of recordings, without reducing the noise on them, to quantify the effect of noise in the manual annotations. The overall result was worse. However, for some recordings, results showed a better performance with the noisy ECG recordings. Specifically, the improvemt in terms of average absolute error with respect to the manual annotations with noise was achieved for P-wave onset, P-wave peak and P-wave offset in the 45.83%, 57.29% and 56.25% of the recordings, respectively.

5.2 Discussion

5.2.1 Results assessment

The delineation result on the QTDB recordings has demonstrated that the proposed method provides a good solution for the accurate delineation of a wide variety of different P-waves morphologies. Specifically, for this work, more than 3000 waveforms from 96 different manually annotated recordings specifically selected to reflect the real world variability has been used. In Table 5.1 apart from the delineation results achieved by the proposed method, other results from relevant delineation methods are shown. In the comparison with them it can be observed how this method outperforms the others in terms of standard deviation and sensitivity. Moreover, the results of standard deviation obtained are also below the acceptable tolerance limits established by the CSE working group for both P-wave onset and offset, also shown in Table 5.1. On the other hand, the average error obtained is in some cases slightly worse in comparison with other methods. However, this worsening can not be considered particularly significant, since results can benefit from the compensation between earlier and later detections with respect to the manual reference. This limitation could be easily overcome if the absolute difference between the automatic and manual annotation were considered as the standard validation parameter instead. However, to allow a fair comparison with other P-wave delineation methods it has been used a validation procedure in the same standard terms.

5.2.2 Selection of other P-wave delineation methods for comparison

For the result comparison, there have been selected among all delineation methods presented in the literature, some of the most relevant. They have been selected to represent the wide variety of strategies employed for P-wave delineation. For instance, from the whole collection of methods making use of

the wavelet transform, Martínez et al. [53] has been selected as it is the most recognized one. However, the wavelet transform has an intrinsic loss of time resolution in the growing scales [84] that might be a decisive drawback for its use in ECG waveform delineation, as well as the high requirements of time and cost that has to be satisfied due to the great amount of calculations needed [85]. The time demand and computational cost is also one of the main disadvantage for the use of statistical and probabilistic methods such as [58,62], which in some cases even need a previous training step. Some other methods have not been included in the comparison because the lack of information about some of the fiducial points considered for this work [29, 61] or due to the reduced number of beats processed [59]. Also, some other methods have not provided any validation result [49, 60].

In a recent paper [30], a comparison between some of the aforementioned algorithms for ECG delineation has been published, assessing their performance by comparing the self-obtained delineation results of each one with the manual annotations of the QTDB. However, the results that are shown for each method are, at least, debatable, as in some cases the exact reproducibility of the algorithms might be impractical due to the lack of some explicit details.

5.2.3 Method improvements

The first meaningful difference between the delineation algorithm presented in this work and others is the high frequency denoising technique applied. Most methods in the literature [29, 59, 63] present a much more aggressive filtering of the ECG signal due to the usual consideration that the normal P-wave spectral characteristic to be limited to low frequencies (10-15 Hz) [7]. However, it has been demonstrated the existence of much higher frequency components in the P-wave [7]. Also, some studies have emphasized the major role that P-wave higher frequency components play when an AF episode approaches [86], which seems to be particularly relevant for this work purpose. This evidence, together with the consequent reduction of the transient effects aggravated by the proximity of the QRS complex, guided the decision of applying a smoother filtering approach.

Some novel strategies had to be implemented in order to perform an accurate delineation of waveforms with a more authentic, and consequently complex, morphology, due to the aforementioned less aggressive filtering. The Gaussian modeling of each P-wave and its subsequent delineation has demostrated to be fairly helpful for guiding the process of locating the boundaries in the original waveform. Also, the morphological information tracking makes the method more robust and consistent.

Another virtue of this method is its simplicity. It does not require a complex mathematical transformation of the signal pattern to locate the fiducial points, like others do [51, 53]. This characteristic makes the method more intuitive and closer to the way of thinking of physicians when delineating ECGs. Therefore, this allows them to take part in decisions about the development of the method itself, as well as possible future improvements.

Also, the novel features introduced as the use of information about previously processed waveforms to guide the delineation of the new ones, allows the monitoring of the morphology trend of the P-waves along the recording. This control over the evolution of the morphological characteristics of these waveforms responds appropriately to the need of detecting changes produced in the signal, as a reflection of possible alteration of the conduction properties of the atria. In addition, the strategy of controlled update of parameters adopted, supports the detection of both progressive changes in P-wave morphology and individual abnormal waveforms.

5.2.4 Criticism of the validation database

One limitation of the presented study is the use of only one annotated database to assess the performance of the proposed method. There are other standard databases containing manual annotation on the P-waves limits, as it was already exposed. Among all those enunced, some were freely available databases, such as the CSEDB [75], which comparatively has a reduced number of P-wave boundaries manual annotations, and the CCDD [76]. These followed the same full-scope annotation than the QTDB. This manual annotation stategy consists in selecting a common point for all leads in sigth. For mono-channel delineation algorithms, such as the presented in this work, this is a major drawback, as no information is provided about which particular wave was taken into account for each annotation and the waveform limits may differ depending on the lead taken into account. So, for the CSEDB and CCDD this handicap gets worse as more leads are provided. In addition, the QTDB has been taken as reference by most P-wave delineation methods, so its use allows a fair performance comparison with them [30].

However, the accuracy of part of the manual annotations in this database have been questioned, specially in those recordings with a lower signal-to-noise ratio (SNR) [29]. The improvement that have been achieved in some recordings when the delineation method was applied without the signal conditioning phase reflects the importance that had noise in the annotation procedure. In addition,

also unclear annotation criteria and significant inaccuracy in the location of boundaries of part of the QTDB P-waves reduce the reliability of the delineation results presented by any algorithm. Even, they could have been developed *ad hoc* and benefit from theses inaccurate annotations [87]. As this fact resulted to be critical for the annotations quality, an alternative accurately annotated database as standard reference for the evaluation of P-wave delineation methods is needed [87].

Chapter 6

Conclusion, Contribution and Future Work

6.1 Conclusion

In this Master's dissertation a novel P-wave delineation method for single-lead ECG signal has been developed and presented. It is based on the differentiation of the signal and novel features have been introduced such as the use of Gaussian models of the P-wave to assist the delineation process and the use of information about the morphology and location of previously delineated waveforms as an aid for the delineation of every coming P-wave. All these added innovations have been decisive to obtain delineation results with respect to a standard annotated reference database that outperform other published methods. In addition, it is a robust method able to quickly adapt to P-waves with changing morphologies as well to detect anomalous events. Therefore, this method is presented as a valuable tool for the identification of abnormal conduction phenomena in the atria, whether produced progressively or in isolated cases.

6.2 Contributions

The strong interest this algorithm may arouse has led to its presentation to the scientific community. To this respect, several contributions related to this delineation method have been submitted, accepted and presented in national and international conferences. Not only the introduction of the delineation

method itself but also other related works such as an extensive criticism to the manual annotations of the standard QT database have been presented. All these conference papers are listed:

International Conference Papers

- González F., Alcaraz R., Rieta JJ. *"Electrocardiographic P-wave Delineation Based on Adaptive Slope Gaussian Detection"*. In Computing in Cardiology Conference (CinC 2017, Rennes 24-27th Sep., France), IEEE, 2017; [88]

- González F., Alcaraz R., Rieta JJ. *"The physionet QT database: Study on the reliability of P-wave manual annotations under noisy recordings"*. In Computing in Cardiology Conference (CinC 2017, Rennes 24-27th Sep., France), IEEE, 2017; [87]

National Conference Papers

- González F., Alcaraz R., Rieta JJ. *"Método para la Delineación de Ondas P en el ECG Basado en Modelado Gaussiano"*. In Congreso de la Sociedad Española de Ingenieía Biomédica (CASEIB 2017, Bilbao 29th Nov-1st Dec., Spain), 2017;

- González F., Alcaraz R., Rieta JJ. *"Estudio Sobre la Fiabilidad de las Anotaciones en la Base de Datos QT de Physionet"*. In Congreso de la Sociedad Española de Ingenieía Biomédica (CASEIB 2017, Bilbao 29th Nov-1st Dec., Spain), 2017;

These scientific publications can be found at the end of this document in the Apendix section.

6.3 Future work

As commented in the discussion section, due to severals characteristics such as its mathematical simplicity or its adaptive feature, the method presented has a lot of potential for new applications and improvements. First, the aim of this method is to identify a correlation between the progressive advance of cardiac remodeling prior AF with an evoluction of the P-wave morphology. To this respect, the proposed method already keep track of certain morphological parameters used during the delineation process. However, still more morphological information could be extracted from the P-waves and infere the atrial transformation, either to prevent the occurence of an AF episode or evaluate the

need for a clinical action. Nowadays, taking into account the revolution that represents for research the complex statistical analysis, an increase of the parameters studied might be potentially decisive.

This method was intended for single-lead ECG signal processing. Therefore, one possible improvement is to include more leads in the delineation process. This multi-lead algorithm could be addressed so that all leads were treated individually and the resulting information is combined. In addition, this approach would improve the method robustness since for some leads the P-waves are poorly defined, wich is a limitation for their delineation [89].

In conclusion, the presumed next step, apart from the always possible improvements in the performance of the method, is its application in a real clinical context, with signals collected from real patients suffering from atrial remodeling.

Chapter 7

Budget

In Table 7.1, costs associated with this Master Dissertation development are summarized and presented, with taxes included. In Tables 7.2, 7.3 and 7.4, the project budjet is presented in detail, broken down into categories of expediture: personal, hardware and software costs, respectively.

Budget summary (taxes included)	
Personal costs	41235 €
Software costs	363 €
Hardware costs	864 €
Total costs	42462 €

Table 7.1: Budget summary

Note that other costs indirectly associated to this Master Dissertation, such as subcriptions to scientific journals and work facilities amortization, have not been included in this budget analysis due to the difficulty of stimating these costs. Also, conferences attendace costs have not been included since it has been considered more associated with the diffusion of the presented work rather than its development.

Personal cots					
Profile	Labour Time	Cost Per Unit	Cost (without employer's fee)	Employer's fee (37'45%)	Total Cost
Biomedical Engineer	750 h.	40 €/h.	30000 €	11235 €	41235 €
Subtotal without employer's fee					30000 €
Subtotal					41235 €

Table 7.2: Personal costs

Hardware cots						
Description	Equipment cost (without taxes)	Amortization period	Use period	Chargeable Cost (withoout taxes)	Taxes (21%)	Total Chargeable Cost
Personal Computer	1500 €	5 years	1 year	300 €	63 €	363 €
Subtotal without taxes						300 €
Subtotal						363 €

Table 7.3: Hardware costs

Hardware cots						
Program	License cost (without taxes)	Amortization period	Use period	Chargeable Cost (withoout taxes)	Taxes (21%)	Total Chargeable Cost
MATLAB R2016a (4 licenses)	2000 €	Indef.	1 year	500 €	105 €	605 €
OS Microsoft Windows 10 Pro	204'61 €	Indef.	1 year	204'61 €	54'39 €	259 €
Subtotal without taxes						309'61 €
Subtotal						864 €

Table 7.4: Software costs

Glossary of Terms

AF: Atrial Fibrillation

ECG: Electrocardiogram

SNR: Signal to Noise Ratio

AV: Atrioventricular

SA: Sinoatrial

RBB: Rigth Bundle Branch

LBB: Left Bundle Branch

WCT: Wilson Central Terminal

ACC: American College of Cardiology

AHA: American Heart Association

ESC: European Society of Cardiology

AERP: Atrial Effective Refractory Period

SW: Search Window

RSE: Reference Signal Excerpt

RPW: Reference P-Wave

CSEDB: CSE multilead measurement Database

CCDD: Chinese Cardiovascular Disease Database

QTDB: QT Database

Se: Sensitivity

TP: True Positive

FN: False Negative

CincC: Computing in Cardiology Conference

CASEIB: Congreso Anual de la Sociedad Española de Ingeniería Bimomédica

List of Figures

Bibliography

[1] Massimo Zoni-Berisso, Fabrizio Lercari, Tiziana Carazza, and Stefano Domenicucci. Epidemiology of atrial fibrillation: European perspective. *Clinical Epidemiology*, 6:213–20, 2014.

[2] Brian J. Potter and Jacques Le Lorier. Taking the pulse of atrial fibrillation. *Lancet (London, England)*, 386:113–5, 2015.

[3] Farah Pellman, Jason; Sheikh. Atrial fibrillation: Mechanisms, therapeutics, and future directions. *Comprehensive Physiology*, 5:649–65, 2015.

[4] Francesco Violi, Daniele Pastori, and Pasquale Pignatelli. Mechanisms and management of thrombo-embolism in atrial fibrillation. *Journal of Atrial Fibrillation*, 7, 2014.

[5] Paulus Kirchhof, Stefano Benussi, Dipak Kotecha, Anders Ahlsson, Dan Atar, Barbara Casadei, Manuel Castella, Hans-Christoph Diener, Hein Heidbuchel, and Jeroen et al. Hendriks. 2016 ESC guidelines for the management of atrial fibrillation developed in collaboration with EACTS. *European Heart Journal*, 37:2893–2962, 2016.

[6] Azfar Sheikh, Nileshkumar J. Patel, Nikhil Nalluri, Kanishk Agnihotri, Jonathan Spagnola, Aashay Patel, Deepak Asti, Ritesh Kanotra, Hafiz Khan, and Chirag et al. Savani. Trends in hospitalization for atrial fibrillation: epidemiology, cost, and implications for the future. *Progress in Cardiovascular Diseases*, 58:105–16, 2015.

[7] Leif Sörnmo and Pablo Laguna. *Bioelectrical Signal Processing in Cardiac and Neurological Applications*. Biomedical Engineering. Academic Press, Burlington, 2005.

[8] Andreas Bollmann, Daniela Husser, Luca Mainardi, Federico Lombardi, Philip Langley, Alan Murray, José Joaquín Rieta, José Millet, S. Bertil Olsson, Martin Stridh, and Leif Sörnmo. Anal-

ysis of surface electrocardiograms in atrial fibrillation: techniques, research, and clinical applications. *EP Europace*, 8(11):911–926, 2006.

[9] Fabio M. Leonelli, Emanuela T. Locati, Giuseppe Bagliani, Roberto De Ponti, Luigi Padeletti, Laura Cipolletta, and Alessandro Capucci. P wave analysis in the era of atrial fibrillation ablation. *Cardiac Electrophysiology Clinics*, 10:299–316, Jun 2018.

[10] Polychronis E. Dilaveris and John E. Gialafos. Future concepts in P-wave morphological analyses. *Cardiac Electrophysiology Review*, 6(3):221–224, 2002.

[11] Valentin Fuster, Lars E. Rydén, Richard W. Asinger, David S. Cannom, Harry J. Crijns, Robert L. Frye, Jonathan L. Halperin, G. Neal Kay, Werner W. Klein, and Samuel et al. Lévy. ACC, AHA, ESC, guidelines for the management of patients with atrial fibrillation: Executive summary a report of the american college of cardiology american heart association task force on practice guidelines and the european society of cardiology committee. *Circulation*, 104(17):2118–2150, 2001.

[12] Jean-Claude Daubert, Dominique Pavin, Gael Jauvert, and Philippe Mabo. Intra- and interatrial conduction delay: implications for cardiac pacing. *Pacing and Clinical Electrophysiology*, 27:507–25, 2004.

[13] Krupal J. Hari, Thong P. Nguyen, and Elsayed Z. Soliman. Relationship between P-wave duration and the risk of atrial fibrillation. *Expert review of cardiovascular therapy*, 16:837–843, 2018.

[14] Federica Censi, Chiara Ricci, Giovanni Calcagnini, Michele Triventi, Renato P. Ricci, Massimo Santini, and Pietro Bartolini. Time-domain and morphological analysis of the P-wave. Part I: Technical aspects for automatic quantification of P-wave features. *Pacing and Clinical Electrophysiology*, 31:874–83, 2008.

[15] Steven A. Guidera and Jonathan S. Steinberg. The signal-averaged P-wave duration: a rapid and noninvasive marker of risk of atrial fibrillation. *Journal of the American College of Cardiology*, 21:1645–51, 1993.

[16] Kudret Aytemir, Necla Ozer, Enver Atalar, Elif Sade, Serdar Aksoyek, Kenan Ovunc, Ali Oto, Ferhan Ozmen, and Sirri Kes. P-wave dispersion on 12-lead electrocardiography in patients with paroxysmal atrial fibrillation. *Pacing and Clinical Electrophysiology*, 23:1109–12, 2000.

[17] Azfar G. Zaman, R. Archabold Archbold, Gérard Helft, Elizabeth A. Paul, Nicholas P. Curzen, and Peter G. Mills. Atrial fibrillation after coronary artery bypass surgery: a model for preoperative risk stratification. *Circulation*, 101:1403–8, 2000.

[18] Joby Chandy, Toshiko Nakai, Randall J. Lee, Wayne H. Bellows, Samir Dzankic, and Jacqueline M. Leung. Increases in P-wave dispersion predict postoperative atrial fibrillation after coronary artery bypass graft surgery. *Anesthesia and Analgesia*, 98:303–10, 2004.

[19] Marco Budeus, Oliver Felix, Marcus Hennersdorf, Heinrich Wieneke, Raimund Erbel, and Stefan Sack. Prediction of conversion from paroxysmal to permanent atrial fibrillation. *Pacing and Clinical Electrophysiology*, 30:243–52, 2007.

[20] Jonas B. Nielsen, Jørgen T. Kühl, Adrian Pietersen, Claus Graff, Bent Lind, Johannes Struijk, Morten S. Olesen, Moritz F. Sinner, Troels N. Bachmann, and Stig et al. Haunsø. P-wave duration and the risk of atrial fibrillation: Results from the Copenhagen ECG Study. *Heart Rhythm*, 12(9):1887–1895, 2015.

[21] Dirk De Bacquer, Julie Willekens, and Guy De Backer. Long-term prognostic value of P-wave characteristics for the development of atrial fibrillation in subjects aged 55 to 74 years at baseline. *The American Journal of Cardiology*, 100(5):850 – 854, 2007.

[22] Federica Censi, Ivan Corazza, Elisa Reggiani, Giovanni Calcagnini, Eugenio Mattei, Michele Triventi, and Giuseppe Boriani. P-wave variability and atrial fibrillation. *Scientific Reports*, 6, 2016.

[23] Giulio Conte, Adrian Luca, Sasan Yazdani, Maria L. Caputo, François Regoli, Tiziano Moccetti, Lukas Kappenberger, Jean-Marc Vesin, and Angelo Auricchio. Usefulness of P-wave duration and morphologic variability to identify patients prone to paroxysmal atrial fibrillation. *American Journal of Cardiology*, 119(2):275–279, 2017.

[24] Pyotr G. Platonov. P-wave morphology: Underlying mechanisms and clinical implications. *Annals of Noninvasive Electrocardiology*, 17(3):161–169, 2012.

[25] Arturo Martínez, Raúl Alcaraz, and José J. Rieta. Morphological variability of the P-wave for premature envision of paroxysmal atrial fibrillation events. *Physiological Measurement*, 35:1–14, 2014.

[26] Dennis H. Lau, Dominik Linz, Ulrich Schotten, Rajiv Mahajan, Prashanthan Sanders, and Jonathan M. Kalman. Pathophysiology of paroxysmal and persistent atrial fibrillation: Rotors, foci and fibrosis. *Heart, Lung & Circulation*, 26:887–893, 2017.

[27] Rajeev K. Pathak, Michelle Evans, Melissa E. Middeldorp, Rajiv Mahajan, Abhinav B. Mehta, Megan Meredith, Darragh Twomey, Christopher X. Wong, Jeroen M.L. Hendriks, Walter P. Abhayaratna, Jonathan M. Kalman, Dennis H. Lau, and Prashanthan Sanders. Cost-effectiveness and clinical effectiveness of the risk factor management clinic in atrial fibrillation. *JACC: Clinical Electrophysiology*, 2017.

[28] Jared W. Magnani, Mary Ann Williamson, Patrick T. Ellinor, Kevin M. Monahan, and Emelia J. Benjamin. P-wave indices: current status and future directions in epidemiology, clinical, and research applications. *Circulation. Arrhythmia and Electrophysiology*, 2:72–9, 2009.

[29] Gustavo Lenis, Nicolas Pilia, Tobias Oesterlein, Armin Luik, Claus Schmitt, and Olaf Dossel. P-wave detection and delineation in the ECG based on the phase free stationary wavelet transform and using intracardiac atrial electrograms as reference. *Biomedizinische Technik. Biomedical Engineering*, 61:37–56, 2016.

[30] I. Beraza and I. Romero. Comparative study of algorithms for ECG segmentation. *Biomedical Signal Processing and Control*, 34:166–173, 2017.

[31] Jaako Malmivuo and Robert Plonsey. *Bioelectromagnetism - Principles and Applications of Bioeletric and Biomagnetic Fields*. Oxford University Press, 1995.

[32] Arnold M. Katz. *Physiology of the Heart*. Lippincott Williams & Wilkins, 2010.

[33] Richard Klabunde. *Cardiovascular Physiolgy Concepts*. Lippincott Williams & Wilkins, 2011.

[34] Sandee Elaine N., Maieb; Sandee Cohen and Katja Hoehn. *Human anatomy & physiology*. Benjaming Cummings, 2006.

[35] José J. Rieta and Raúl Alcaraz. *The Genesis of the Electrocardiogram (ECG)*. 2017.

[36] S. Serge Barold. Willem Einthoven and the birth of clinical electrocardiography a hundred years ago. *Cardiac Electrophysiology Review*, 7(1):99–104, 2003.

[37] John R. Hampton. *The ECG Made Easy*. Churchill Livingstone, 2003.

[38] Tomas B. Garcia; Neil E. Holtz. *Introduction to 12-Lead ECG: The Art of Interpretation*. Jones & Bartlett Learning, 2003.

[39] Ulin. Schotten, Dobromir. Dobrev, Pyotr G. Platonov, Hans Kottkamp, and Gerhard Hindricks. Current controversies in determining the main mechanisms of atrial fibrillation. *Journal of Internal Medicine*, 279:428–38, May 2016.

[40] Peter Kowey, Jonathan Piccini, Gerald Naccarelli, and James A. Reiffel, editors. *Cardiac Arrhythmias, Pacing and Sudden Death*. Springer International Publishing, 2017.

[41] Michel Haissaguerre, Pierre Jais, Dipen C. Shah, Atsushi Takahashi, Mélèze Hocini, Gilles Quiniou, Stéphane Garrigue, Alain Le Mouroux, Philippe Le Metayer, and Jaques Clementy. Spontaneous initiation of atrial fibrillation by ectopic beats originating in the pulmonary veins. *The New England Journal of Medicine*, 339:659–66, 1998.

[42] Stanley Nattel, Brett Burstein, and Dobromir Dobrev. Atrial remodeling and atrial fibrillation: mechanisms and implications. *Circulation. Arrhythmia and Electrophysiology*, 1:62–73, 2008.

[43] Maurits C. Wijffels, Charles J. Kirchhof, Rick Dorland, and Maurits A. Allessie. Atrial fibrillation begets atrial fibrillation. A study in awake chronically instrumented goats. *Circulation*, 92:1954–68, 1995.

[44] Maurits Allessie, Jannie Ausma, and Ulrich Schotten. Electrical, contractile and structural remodeling during atrial fibrillation. *Cardiovascular Research*, 54:230–46, 2002.

[45] Victor L. Thijssen, Jannie Ausma, and Marcel Borgers. Structural remodelling during chronic atrial fibrillation: act of programmed cell survival. *Cardiovascular Research*, 52:14–24, 2001.

[46] Pyotr G. Platonov. Atrial fibrosis: an obligatory component of arrhythmia mechanisms in atrial fibrillation? *Journal of Geriatric Cardiology*, 14:233–237, 2017.

[47] Yu-ki Iwasaki, Kunihiro Nishida, Takeshi Kato, and Stanley Nattel. Atrial fibrillation pathophysiology. *Circulation*, 124(20):2264–2274, 2011.

[48] Simona Petrutiu, Jason Ng, Grace M. Nijm, Haitham Al-Angari, Steven Swiryn, and Alan V. Sahakian. Atrial fibrillation and waveform characterization. A time domain perspective in the surface ECG. *IEEE Engineering in Medicine and Biology Magazine*, 25:24–30, 2006.

[49] Ivaturi S. Murthy and U. C. Niranjan. Component wave delineation of ECG by filtering in the Fourier domain. *Medical & Biological Engineering & Computing*, 30:169–76, 1992.

[50] Ivatury S. Murthy and Durga G. S. Prasad. Analysis of ECG from pole-zero models. *IEEE Transactions on Bio-Medical Engineering*, 39:741–51, 1992.

[51] Arturo Martínez, Raúl Alcaraz, and José J. Rieta. Application of the phasor transform for automatic delineation of single-lead ECG fiducial points. *Physiological Measurement*, 31(11):1467–1485, 2010.

[52] Cuiwei Li, Chongxun Zheng, and Changfeng Tai. Detection of ECG characteristic points using wavelet transforms. *IEEE Transactions on Biomedical Engineering*, 42(1):21–28, 1995.

[53] Juan P. Martínez, Rute Almeida, Salvador Olmos, Ana P. Rocha, and Pablo Laguna. A wavelet-based ECG delineator evaluation on standard databases. *IEEE Transactions on Biomedical Engineering*, 51(4):570–581, 2004.

[54] Jyotinder S. Sahambi, Shretima N. Tandon, and Rajendra K. P. Bhatt. Using wavelet transforms for ECG characterization. *IEEE Engineering in Medicine and Biology Magazine*, 16(1):77–83, 1997.

[55] Ali Ghaffari, Mohammad R. Homaeinezhad, Mehdi Akraminia, Mohammad Atarod, and Mohammad Daevaeiha. A robust wavelet-based multi-lead electrocardiogram delineation algorithm. *Medical Engineering and Physics*, 31(10):1219–1227, 2009.

[56] Jacques Dumont, Alfredo I. Hernández, and Guy Carrault. Improving ECG beats delineation with an evolutionary optimization process. *IEEE Transactions on Biomedical Engineering*, 57(3):607–615, 2010.

[57] Atiyeh Karimipour and Mohammad R. Homaeinezhad. Real-time electrocardiogram P-QRS-T detection-delineation algorithm based on quality-supported analysis of characteristic templates. *Computers in Biology and Medicine*, 52:153–165, 2014.

[58] H. J. L. M. Vullings, Michel H. G. Verhaegen, and H. B. Verbruggen. Automated ECG segmentation with dynamic time warping. In *Proceedings of the 20th Annual International Conference of the IEEE Engineering in Medicine and Biology Society.*, pages 163–166, 1998.

[59] Ali Zifan, Sohrab Saberi, Mohammad Hassan Moradi, and Farzad Towhidkhah. Automated ECG segmentation using piecewise derivative dynamic time warping. In *International Journal of Biomedical Sciences, 1*, pages 181–185, 2006.

[60] Nicholas P. Hughes, Lionel Tarassenko, and Stephen J. Roberts. Markov models for automated ECG interval analysis. *Advances in Neural Information Processing Systems*, 2004.

[61] Rodrigo Andreão, Bernadette Dorizzi, and Jérôme Boudy. ECG Signal Analysis through Hidden Markov Models. *IEEE transactions on bio-medical engineering*, 53:1541–9, 09 2006.

[62] Chao Lin, Corinne Mailhes, and Jean-Yves Tourneret. P- and T-wave delineation in ECG signals using a bayesian approach and a partially collapsed gibbs sampler. *IEEE Transactions on Biomedical Engineering*, 57(12):2840–2849, 2010.

[63] Pablo Laguna, Raimon Jané, and Pere Caminal. Automatic detection of wave boundaries in multilead ECG signals: Validation with the CSE database. *Computers and Biomedical Research*, 27(1):45–60, 1994. ANSI/AAMI, Testing and reporting performance results of cardiac rhythm and ST segment, ANSI/AAMI EC 57-293, 1998, p. 37.

[64] Yogendra N. Singh and Phalguni Gupta. ECG to individual identification. In *IEEE 2nd International Conference on Biometrics: Theory, Applications and Systems*, 2008.

[65] Nourhan Bayasi, Temesghen Tekeste, Hani Saleh, Ahsan Khandoker, Baker Mohammad, and Mohammed Ismail. Adaptive technique for P and T wave delineation in electrocardiogram signals. In *Annual International Conference of the IEEE Engineering in Medicine and Biology Society.*, volume 2014, pages 90–93, 2014.

[66] Suzanna M. M. Martens, Massimo Mischi, Guid Oei, and Jan W. M. Bergmans. An improved adaptive power line interference canceller for electrocardiography. *IEEE Transactions on Biomedical Engineering*, 53:2220 – 2231, 2006.

[67] Manuel García, Miguel Martínez-Iniesta, Juan Ródenas, José J Rieta, and Raúl Alcaraz. A novel wavelet-based filtering strategy to remove powerline interference from electrocardiograms with atrial fibrillation. *Physiological Measurement*, 39(11):115006, nov 2018.

[68] Md. Ashfanoor Kabir and Celia Shahnaz. Denoising of ECG signals based on noise reduction algorithms in EMD and wavelet domains. *Biomedical Signal Processing and Control*, 7(5):481 – 489, 2012.

[69] Yan Sun, Kap Luk Chan, and Shankar Muthu Krishnan. ECG signal conditioning by morphological filtering. *Computers in Biology and Medicine*, 32(6):465–479, 2002.

[70] Bert-Uwe Kohler, Carsten Hennig, and Reinhold Orglmeister. The principles of software QRS detection. *IEEE Engineering in Medicine and Biology Magazine*, 21:42–57, 2002.

[71] Heike Leutheuser, Stefan Gradl, Lars Anneken, Martin Arnold, Nadine Lang, Stephan Achenbach, and Bjoern M. Eskofier. Instantaneous P- and T-wave detection: Assessment of three ECG fiducial points detection algorithms. In *IEEE 13th International Conference on Wearable and Implantable Body Sensor Networks (BSN)*, pages 329–334, 2016.

[72] Geroge B. Moody and Roger G. Mark. The impact of the MIT-BIH arrhythmia database. *IEEE Engineering in Medicine and Biology Magazine*, 20:45–50, May-Jun 2001.

[73] Mohamed Elgendi, Bjoern Eskofier, and Derek Abbott. Fast T wave detection calibrated by clinical knowledge with annotation of P and T waves. *Sensors*, 15:17693–714, Jul 2015.

[74] Alessandro. Taddei, G. Distante, Michele Emdin, P. Pisani, G. B. Moody, C. Zeelenberg, and C. Marchesi. The European ST-T database: standard for evaluating systems for the analysis of ST-T changes in ambulatory electrocardiography. *European Heart Journal*, 13:1164–72, Sep 1992.

[75] Jos L. Willems, Pierre Arnaud, Jan H. van Bemmel, Peter J. Bourdillon, Rosansa Degani, Bernard Denis, Ian Graham, Frits M. Harms, Peter W. Macfarlane, and Gianfranco Mazzocca. A reference data base for multilead electrocardiographic computer measurement programs. *Journal of the American College of Cardiology*, 10:1313–21, Dec 1987.

[76] Jia-Wei Zhang, Xia Liu, and Jun Dong. Ccdd: An enhanced standard ecg database with its management and annotation tools. *International Journal on Artificial Intelligence Tools*, 21(05):1240020, 2012.

[77] Pablo Laguna, Daniel S. Goldberg, and George B. Moody. A database for evaluation of algorithms for measurement of QT and other waveform intervals in the ECG. In *Computers in Cardiology*, 1997.

[78] Luigi Y. Di Marco and Lorenzo Chiari. A wavelet-based ECG delineation algorithm for 32-bit integer online processing. *Biomedical engineering online*, 10:23, Apr 2011.

[79] *ANSI/AAMI, Testing and reporting performance results of cardiac rhythm and ST segment*. ANSI/AAMI EC 57-293, 1998.

[80] François Portet. P wave detector with PP rhythm tracking: evaluation in different arrhythmia contexts. *Physiological Measurement*, 29(1):141–155, jan 2008.

[81] Nicolas Boichat, Nadia Khaled, Francisco Rincon, and David Atienza. Wavelet-based ECG delineation on a wearable embedded sensor platform. *Sixth International Workshop On Wearable And Implantable Body Sensor Networks, Proceedings*, pages 256–261, 2009.

[82] The CSE Working Party. recommendations for measurement standards in quantitative electrocardiography. *European heart journal*, 6:815–25, Oct 1985.

[83] F. Rincón, J. Recas, N. Khaled, and D. Atienza. Development and evaluation of multilead wavelet-based ecg delineation algorithms for embedded wireless sensor nodes. *IEEE Transactions on Information Technology in Biomedicine*, 15(6):854–863, 2011.

[84] Rute Almeida, Juan Pablo Martinez, Salvador Olmos, Ana Paula Rocha, and Pablo Laguna. Automatic delineation of T and P waves using a wavelet-based multiscale approach. In *1st International Congress on Computational Bioengineering*, pages 243–247, 2003.

[85] Sunil Patil and Eric W. Abel. Real time continuous wavelet transform implementation on a DSP processor. *Journal of Medical Engineering & Technology*, 33(3):223–231, 2009.

[86] Raúl Alcaraz, Arturo Martínez, and José J. Rieta. Role of the P-wave high frequency energy and duration as noninvasive cardiovascular predictors of paroxysmal atrial fibrillation. *Computer Methods and Programs in Biomedicine*, 119:110–9, Apr 2015.

[87] Francisco González, Raúl Alcaraz, and José J. Rieta. The physionet QT database: Study on the reliability of P-wave manual annotations under noisy recordings. In *Computing in Cardiology*, 2017.

[88] Francisco González, Raúl Alcaraz, and José J. Rieta. Electrocardiographic P-wave delineation based on adaptive slope Gaussian detection. In *Computing in Cardiology*, 2017.

[89] Rute Almeida, Juan Pablo Martínez, Ana Paula Rocha, and Pablo Laguna. Multilead ecg delineation using spatially projected leads from wavelet transform loops. *IEEE Transactions on Biomedical Engineering*, 56(8):1996–2005, Aug 2009.

Appendix

The next pages include two International Conference Papers and two National Conference Papers derived from this Master's Dissertation, as described in section 6.2.

- González F., Alcaraz R., Rieta JJ. *"Electrocardiographic P-wave Delineation Based on Adaptive Slope Gaussian Detection"*. In Computing in Cardiology Conference (CinC 2017, Rennes 24-27th Sep., France), IEEE, 2017; [88].

- González F., Alcaraz R., Rieta JJ. *"The physionet QT database: Study on the reliability of P-wave manual annotations under noisy recordings"*. In Computing in Cardiology Conference (CinC 2017, Rennes 24-27th Sep., France), IEEE, 2017; [87].

- González F., Alcaraz R., Rieta JJ. *"Método para la Delineación de Ondas P en el ECG Basado en Modelado Gaussiano"*. In Congreso Anual de la Sociedad Española de Ingenieía Biomédica (CASEIB 2017, Bilbao 29th Nov-1st Dec., Spain), 2017.

- González F., Alcaraz R., Rieta JJ. *"Estudio Sobre la Fiabilidad de las Anotaciones en la Base de Datos QT de Physionet"*. In Congreso Anual de la Sociedad Española de Ingenieía Biomédica (CASEIB 2017, Bilbao 29th Nov-1st Dec., Spain), 2017.

Electrocardiographic P-wave Delineation Based on Adaptive Slope Gaussian Detection

Francisco González[1], Raúl Alcaraz[2], José J Rieta[1]

[1] BioMIT.org, Electronic Engineering Department, Universitat Politecnica de Valencia, Spain
[2] Research Group in Electronic, Biomedical and Telecomm. Eng., Univ. of Castilla-La Mancha, Spain

Abstract

The study of the P-wave on the electrocardiogram is essential in the characterization of atrial conduction defects that may anticipate cardiac pathologies, such as atrial fibrillation. This evidence exhibits the need to develop reliable methods for accurate automatic delineation of P-waves. Many different strategies for delineating P-waves have been introduced. Nonetheless, they all share the same principle of smoothing aggressively the P-wave pattern to facilitate its delineation. However, that strategy may provoke morphological alterations in the P-wave under study that could lead to inaccurate delineation. Alternatively, the present work introduces a new delineation strategy grounded on the generation of a Gaussian model of the P-wave under study to assist its delineation and an adaptive slope threshold that takes into account the morphology of the preceding P-waves. The method was validated using the annotated QT database from Physionet. Delineation results provided a detection sensitivity of 100%, whereas the mean and standard deviation of the delineation error for the P-wave onset, peak and offset were 4.71 ± 9.59 *ms,* 2.82 ± 6.69 *ms and* 0.6 ± 9.79 *ms, respectively. These results demonstrate that the proposed strategy provides accurate delineation of P-waves that outperforms others presented in the literature, in particular in terms of stability.*

1. Introduction

The P-wave on the electrocardiogram (ECG) represents the electrical activity of the atria and is considered the most reliable non-invasive source of information about atrial conduction [1]. Some morphology characteristics of the P-wave such as its maximum duration or dispersion, among others, have been associated to a higher recurrence and incidence of Atrial Fibrillation (AF), the most common arrhythmia [2]. However, the extraction of information as the boundaries of these waveforms is a complex task due to the absence of standard measurement techniques [2] and the lack of a consensus about the precise definition of the location of these points in the ECG signal. Moreover, manual delineation is a time consuming task with inaccurate results that may vary significantly as a function of the experience and/or fatigue of the physician as well as the presence of noise within the signal [3]. Consequently, this fact has motivated the development of a wide variety of automatic P-wave delineation methods based on different principles. The strategies followed by them range from the use of mathematical tranforms as the phasor transform [4] or the wavelet transform [3, 5] to the differentiation of the ECG signal [6], among others.

The method proposed in this study is based on the differentiation of the signal as proposed by Laguna et al. [6], but with decisive differences as the calculation of an adaptive slope threshold that takes into account the morphological characteristics of the preceding P-waves and the creation of a Gaussian model of every P-wave to assists its delineation. In this way, it has been designed an algorithm capable of detecting and delineating accurately a wide variety of P-wave shapes which, in addition, is more respectful with the morphology of the waveforms and more stable than other methods presented in the literature.

2. Methods

2.1. Dataset and preprocessing

For validation purpose in this study it has been used the standard QT Database (QTDB) [7]. This database contains 105 fifteen-minutes two leads ECG recordings collected from other existing databases with at least 30 manually annotated beats per recording. This database has been chosen as the reference for other P-wave delineator developers for presenting a wide variety of P-wave morphologies and being almost the only free available standard database that contains manual P-wave boundaries annotations. Even though, the lack of accuracy of these annotations, declared as performed at full scope of the two available leads, has been questioned in several previous studies. One recent example can be found in [3].

 ISSN: 2325-887X DOI:10.22489/CinC.2017.236-033

Before the proposed delineation method is applied, the input ECG must be properly conditioned. Initially, the signal is resampled up to 1 kHz, the base line is eliminated by subtracting the signal envelope and the power line interference frequency component is removed through adaptive filtering. Later, the high frequency muscle noise is reduced first by applying a wavelet-based method and a bidirectional low-pass filter. The cut-off frequency selected was 70 Hz, a less aggressive filtering than other comparable methods [3, 6]. This option responds to the demonstrated existence of much higher frequency components in the P-wave than the usually considered [8] and a reduction in the transient effect produced by the proximity of the QRS complex. The last step of the preprocessing is a supervised location of the R-peaks within the signal [9].

2.2. Delineation algorithm

In the proposed method, each P-wave is not delineated independently. Instead of that, certain parameters calculated from previously delineated waveforms are used as previous information to guide the location of the fiducial points within a P-wave. Consequently, an initialization step is needed at the beginning of the delineation process in which these parameters are obtained from a reference P-wave, which construction is described next.

2.3. Reference P-wave construction

Initially, signal segments prior to the first five R-peaks previously detected are averaged to create a reference segment of the signal. From this, the QRS onset is estimated first and then, prior that point, in a search window of length equal to one third of the median RR distances, the peak with greater amplitude is sought. This point is labelled as the reference P-wave peak. Around that position, a segment of 180 ms in length is isolated, and will serve as the reference P-wave. Extraordinarily, if the median RR interval is too long (>900 ms) or too short (<600 ms) this length is increased or reduced by 20 ms, respectively.

This constructed P-wave might be first categorized as monophasic positive, monophasic negative or biphasic (positive–negative or negative–positive). To do so, a decision algorithm is performed as follows. First, a Gaussian function is generated so that it fits the P-wave in the best way possible. If the fit is good enough, statement that for this method is translated as a Pearson correlation coefficient greater than 0.7, the waveform is determined to be monophasic positive. Otherwise, the procedure is repeated with the P-wave inverted. In case a proper fit is obtained now, the waveform is classified as monophasic negative. Finally, in case of a new mismatch the waveform is classified as biphasic. For this latter case, the two peaks of the biphasic P-wave are sought forward and backward and the P-wave window is recentered to fit the biphasic morphology. Furthermore, a new Gaussian model to better fit the biphasic wave is created by increasing the order of the Gaussian function. This order is augmented until a Pearson correlation between the P-wave and the Gaussian function higher than 0.7 is reached.

It might be noticed that some P-waves can be asymmetrical. In those cases the Gaussian model will not fit acceptably in any case, which may compromise the delineation performance. When this occur, each half of the P-wave is delineated independently by constructing two artificial waveforms. This is done by meeting both halves with themselves mirrored. Then the delineation of just one half of those artificial waveforms is carried out, as they were distinct P-waves.

To determine the boundaries of the waveform, the Gaussian function is differentiated first and then, the maximum values in each half of the wave are identified, which are the points in which the Gaussian function presents its maximum slopes. Later, based on those values, a slope threshold is calculated and the boundaries of the waveform are determined as the points in which the threshold is exceeded. To determine the mathematical relationship between the maximum slope of a waveform and the slope in its boundaries in each case, a total of 60 P-waves were manually delineated by two expert physicians. Thus, this relationship was plotted and the function that resulted to be the best fit, with an R-square score of 0.815, was simplified to obtain the following equation defining the threshold:

$$Th(x) = \frac{0.0058 \cdot x}{x + 0.012}, \tag{1}$$

where x stands for the waveform maximum slope.

After the Gaussian function has been delineated, the process is repeated with the real P-wave, but restricting the search area for each fiducial point to the vicinity of their position in the model wave. Figure 1 plots an example of this situation in which these intervals are colored in gray. The width of the regions around each fiducial point depends on the goodness of the Gaussian fit. Thus, Figure 1 shows how the area around the offset of the Gaussian model is wider (see offset of this P-wave) as the fit is worse in that half of the wave.

In summary, from the representative P-wave already delineated, the following information is obtained: differences in time and amplitude between the maximum peak of the waveform and its boundaries, the approximated position of the wave with respect to the R-peak, the width of the search window (defined as the width of the waveform, widened a quarter of it on each side), the type of the waveform morphology and some starting coefficients for the Gaussian fit. All this knowledge about the morphology of the P-wave taken as reference will be used to ease the delineation of the P-waves individually.

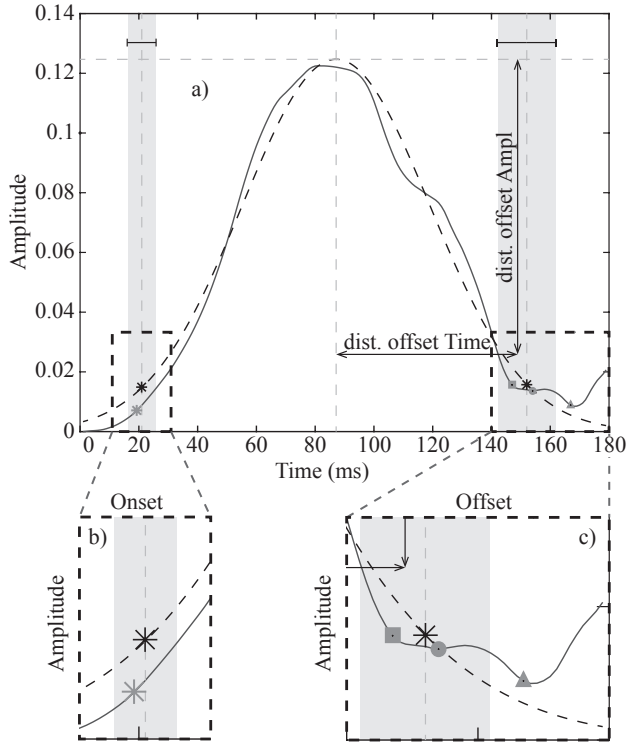

Figure 1. Real P-wave (solid line) and its Gaussian model (dotted line). (a) The detected boundaries on the Gaussian waveform are indicated as black asterisks. The fiducial points search interval is shaded in grey around them. Reference distances in time and amplitude between the peak and the offset computed by taking into account previous waveform morphologies are also displayed. (b) Enlarged beginning with a grey asterisk detected in the real wave as candidate for P-wave onset. (c) Enlarged wave end with different grey shapes are the candidates for P-wave offset.

2.4. Individualized P-wave delineation

With all the information obtained from the initialization step, every P-wave is detected in its corresponding search window prior to the R-peak. The delineation method is basically in the same as described before for the reference P-wave. The only difference is the possible existence of more than one fiducial point candidate. In that case, the final decision is based on the morphology parameters that were calculated during the initialization phase. This circumstance is also illustrated in Figure 1.c, where three offset candidates are represented as different grey geometric figures. First, the triangle option would be discarded as it is outside the restricted interval. And then, between the two remaining options, the square option would be selected as it is closer to the point determined by the morphology parameters: distances from peak to offset in time and amplitude obtained from previously delineated P-waves.

Table 1. Comparison of the delineation performance of some of the most relevant P-wave delineation methods in the literature by means of two Validation Parameters (V.P.) making use of the QTDB.

Methods	V. P.	P_{ON}	P_{PEAK}	P_{OFF}
This method	Se(%)	100	100	100
	$\mu \pm \sigma$(ms)	4.7±9.6	2.8±6.7	0.6±9.8
A. Martínez	Se(%)	98.65	98.65	98.65
et al. [4]	$\mu \pm \sigma$(ms)	2.6±14.5	32±25.7	0.7±14.7
J.P. Martínez	Se(%)	98.87	98.87	98.87
et al. [5]	$\mu \pm \sigma$(ms)	2.0±14.8	3.6±13.2	1.9±12.8
P. Laguna	Se(%)	97.7	97.7	97.7
et al. [6]	$\mu \pm \sigma$(ms)	14±13.3	4.8±10.6	−0.1±12.3

Ultimately, once the new P-wave has been delineated, all the parameters obtained which are associated to the reference P-wave are also recomputed with the aim to update some possible variations. An influence ratio of 20% over the total has been considered. However, before the computations are made, every pair of values are compared. In case the difference is sufficiently large ($> 25\%$), the wave is labeled as abnormal and the refreshing procedure for the reference P-wave is aborted.

3. Results

To asses the performance of the proposed algorithm, the delineation error was computed as the difference in time between automatic delineation and manual annotations in the QTDB. For each recording, the larger set of manual annotations in the database was considered. Thus, the global score is presented in terms of the average value of the error (μ) and its standard deviation (σ) as proposed by Martínez et al. [5]. Also the detection performance is evaluated by its Sensitivity (Se%). This parameter indicates the percentage of well detected events. Table 1 shows the results of the proposed method in comparison with other relevant methods presented in the literature.

Results of the proposed method in Table 1 were obtained by using a total of 3176 annotated beats from 96 of the 2-leads ECG recordings from the QTDB. From the original set of 105 recordings, seven of them (*sel102*, *sel221*, *sel232*, *sel310*, *sel36*, *sel37*, *sel50*) were excluded for the delineation as no P-wave manual annotation were provided and also recordings *sel104* and *sel36* were not delineated as they did not present a minimum of three consecutive annotated P-waves, a self-imposed condition.

4. Discussion

The delineation results on the QTDB shown in Table 1 have demonstrated that the proposed method is capable of accurately delineate a wide variety of different P-wave morphologies. This has been shown by the more than 3000 waveforms delineated from a large amount of different manually annotated recordings specifically selected to reflect the real world variability. Moreover, it is important to note the excellent results achieved in terms of the standard deviation of the error and sensitivity. It can be observed how the proposed delineation method outperforms the other methods in terms of these two variables. In addition, both for P-wave onset and offset, the obtained standard deviation values are below the acceptable tolerance limits stablished by the CSE working group [10], that are, respectively, 10.2 and 12.7 ms. This exhibits the great stability that brings the use of Gaussian models of the P-waves as delineation assistants.

On the other hand, with respect to the average value of the error the score obtained, even if still satisfactory, is improved in some cases for those presented by other methods. However, this standard validation parameter might be misleading, since it is likely to benefit from the compensation between earlier and later detections. This risk could be avoided if the mean absolute error was considered instead. Unlike other methods that are based in the use of complex transforms [3–5], the proposed strategy is completely developed in the time domain. This option could be considered more intuitive as it is closer to the way of thinking of physicians when delineating ECGs and, therefore, it could allow the developers to receive feedback more easily for the future improvements of the algorithm.

5. Conclusions

In this study, an adaptive P-wave delineation method based on the differentiation of the signal has been presented. The use of information about the historical morphology of the P-waves already delineated and the creation of Gaussian models of every single P-wave to assist its delineation have been revealed as key factors providing higher delineation accuracy and better stability to abnormal P-waves, thus outperforming other methods presented in the literature. Moreover, this algorithm allows a monitoring of the P-wave morphology trend along the ECG and detect anomalous events. Therefore, this method could represent a potencial solution for the identification of progressive changes in the electrical properties of the atria which may help to foresee the occurrence of episodes of arrhythmias, such as atrial fibrillation, or in the clinical decision-making with respect to the diagnosis of cardiovascular diseases related with atrial conduction defects.

Acknowledgements

Research supported by grants TEC2014–52250–R and DPI2017–83952–C3 MINECO/AEI/FEDER, UE.

References

[1] Platonov PG. Atrial conduction and atrial fibrillation: What can we learn from surface ECG? Cardiology Journal 2008; 15(5):402–407.

[2] Magnani JW, Williamson MA, Ellinor PT, Monahan KM, Benjamin EJ. P-wave indices: current status and future directions in epidemiology, clinical, and research applications. Circulation Arrhythmia and electrophysiology Feb 2009;2:72–9.

[3] Lenis G, Pilia N, Oesterlein T, Luik A, Schmitt C, Dössel O. P-wave detection and delineation in the ECG based on the phase free stationary wavelet transform and using intracardiac atrial electrograms as reference. Biomedizinische Technik 2016;61(1):37–56.

[4] Martínez A, Alcaraz R, Rieta JJ. Application of the phasor transform for automatic delineation of single-lead ECG fiducial points. Physiological Measurement 2010; 31(11):1467–1485.

[5] Martínez JP, Almeida R, Olmos S, Rocha AP, Laguna P. A wavelet-based ECG delineator evaluation on standard databases. IEEE Transactions on Biomedical Engineering 2004;51(4):570–581.

[6] Laguna P, Jané R, Caminal P. Automatic detection of wave boundaries in multilead ECG signals: Validation with the CSE database. Computers and Biomedical Research 1994; 27(1):45–60.

[7] Laguna P, Mark RG, Goldberg A, Moody GB. Database for evaluation of algorithms for measurement of QT and other waveform intervals in the ECG. In Computers in Cardiology. 1997; 673–676.

[8] Sörnmo L, Laguna P. Chapter 6 - the electrocardiogram-a brief background. In Bioelectrical Signal Processing in Cardiac and Neurological Applications, Biomedical Engineering. Burlington: Academic Press. ISBN 978-0-12-437552-9, 2005; 411 – 452.

[9] Kohler B, Hennig C, Orglmeister R. The principles of software QRS detection. Engineering in Medicine and Biology Magazine IEEE 2002;21(1):42–57.

[10] The CSE working party. Recommendations for measurement standards in quantitative electrocardiography. European heart journal Oct 1985;6:815–25.

Address for correspondence:

Francisco González Molina
Electronic Engineering Department, Building 7F
Universidad Politécnica de Valencia
Camino de Vera, s/n, 46022, Valencia, Spain
E-mail: fgmolina@upv.es

The Physionet QT Database: Study on the Reliability of P-wave Manual Annotations Under Noisy Recordings

Francisco González[1], Raúl Alcaraz[2], José J Rieta[1]

[1] BioMIT.org, Electronic Engineering Department, Universitat Politecnica de Valencia, Spain
[2] Research Group in Electronic, Biomedical and Telecomm. Eng., Univ. of Castilla-La Mancha, Spain

Abstract

Thanks to its manual annotations, the PhysioNet QT database (QTDB) has been widely used as the reference of ECG delineators. However, a significant percentage of its annotations have been reported as inaccurate. Thus, any precise ECG delineator will never be able to meet, without error, all its annotations. The present work analyzes these inaccuracies and also how noise altered the final timing of annotations. As this effect is higher for low amplitude waveforms, P-waves were studied through a robust P-wave delineator. Its delineation results were compared with manual annotations under two scenarios. Firstly, a direct comparison without ECG denoising was performed. Secondly, the P-waves were delineated after efficient Wavelet-based denoising. Results showed that automatic annotations were closer to manual annotations for noisy ECGs and farther in the case of denoised ECGs, thus proving that noise altered the timing of manual annotations. An unreal improvement in delineation performance for noisy ECGs was obtained for P-wave onset, peak and offset in 45.83%, 57.29% and 56.25% of the recordings, respectively. Thus, to improve delineators reliability, either the need to review the QTDB annotations or its replacement by a better annotated database are suggested.

1. Introduction

Any new ECG signal processing algorithm designed to be used in a clinical setting requires the evaluation of its performance [1]. To do so, as well as for its proper development, the availability of databases, whose size is large enough to cover the wide diversity of waveform patterns that ECG recordings may present, is required [1]. Moreover, for the validation of some specific methods such as detectors or delineators of particular waves, annotations defining the time instants when these events occur are needed. In order to consider these annotations trustworthy, they might be determined manually and carefully by expert physicians. However, there exist many factors that can influence the result of these manual annotations and, therefore, compromise their reliability.

There exist a considerable number of standard databases available to researchers with their proper distinctive features that depend on the initial aim for which they were created. Two of these databases are the MIT-BIH arrhythmia database [2] and the AHA Database, which were developed to evaluate arrhythmia detectors. On the other hand, the European ST-T Database was born in response to the growing interest in the analysis of ST-T segment as indicative of myocardial ischemia [3]. However, none of the aforementioned databases contains manual annotations of the locations of boundaries and peaks of all the waveforms that can be found in a normal ECG recording, something necessary for the validation of delineation methods of these waves. Therefore, standard databases providing manual annotations of ECG waves boundaries and peaks are needed. Some examples of this are the CSE multilead measurement database (CSEDB) [4] and the QT-database (QTDB) [5]. However, due to its free access and mirrored availability, this latter database has been the most widely used as a reference for the validation of P-wave delineation algorithms during last years.

Furthermore, the additional characteristics that have caused the QTDB to reach that position are, mainly, the wide diversity of waveform morphologies that contains, as recordings were specifically selected to reflect the real world variability and the considerable amount of waveforms annotations made manually by expert physicians, much more than in the CSEDB. In addition, another significant difference between these two databases is that the QTDB is public, thus allowing any researcher to use it without the need of financial support. However, manual annotations may not always be perfectly accurate. In this study the quality of manual waveform timings in the QTDB has been evaluated, specifically for the case of the P-waves, and the origin of the possible errors in the precise location of these points has been analyzed.

 ISSN: 2325-887X DOI:10.22489/CinC.2017.255-156

2. The QT database

The QTDB consists of 105 fifteen-minutes excerpts of two channels ECG recordings. These signals were collected from other existing databases as the MIT-BIH Arrhythmia Database and the European ST-T Database, as well as other databases collected at Bostons's Beth Israel Hospital. It contains manual annotations of the beginning, peak and end of P-waves; beginning and end of QRS-complexes; peak and end of T-waves and, if present, the peak and end of U-waves. These annotations are present in, at least, 30 beats per record. The annotated beats were selected among the signal to represent its more characteristic or dominant morphological pattern [5].

The QTDB contains two sets of manual annotations made by each expert physician. However, one of them include annotations for just 11 records and, consequently, has rarely been used for validation purposes. Hence, in this study only the larger set of annotation will be discussed.

The process of manually annotating a signal is a complex, time consuming task. In addition, variables as the experience of the annotator, the degree of concentration and tiredness during the accomplishment of the task or the annotation tool accuracy and reliability, among others, can influence in the outcome of the procedure. Moreover, the presence of noise in the signal may further complicate this task, especially for low amplitude waves such as the P-wave. Due to this evidence, and the increasing attention that has gained the delineation of P-waves within the ECG because of the demonstrated relationship between different morphological characteristics of this waveform and clinical conditions, such as the recurrence of atrial fibrillation [6], the P-wave in particular has been selected in this study to evaluate the accuracy or the QTDB manual annotations.

3. Reliability analysis of the QTDB

3.1. The full scope concern

During the manual annotation process of the QTDB both leads were displayed simultaneously and the location of the annotations was established common to both channels [5]. This adopted procedure presents a serious drawback when it comes to knowing which wave was taken into account for each particular annotation, which is basic for the validation of single-lead delineation algorithms. In fact, due to the projection of the cardiac vector under each lead, it is well known that the ECG waves timing will be different as a function of the considered lead [7].

Other recently available database, the Chinese Cardiovascular Diseases Database (CCDD) [8], has followed the same full-lead scope annotation procedure, in which the annotation of boundaries and peaks positions are common

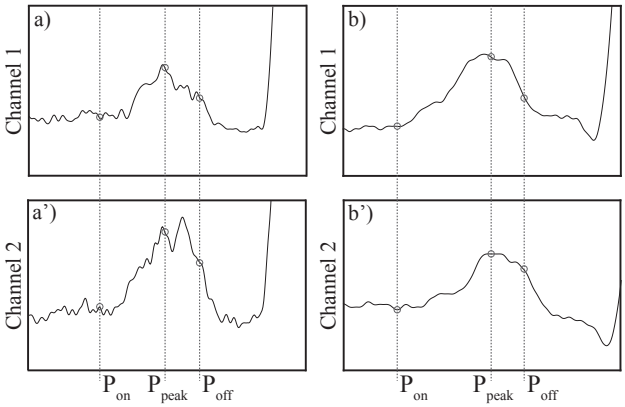

Figure 1. Examples of arguable annotated P-waves from the QTDB. a) and a') show the P-wave in both channels corresponding to the 17^{th} annotated beat from recording *sele303*. b) and b') show both channels of the 17^{th} annotated beat in recording *sel33*. The full scope fiducial points locations are indicated with a dotted line. Remark that, specially the offset annotations, are more than debatable.

for all leads. This specific case is even more challenging to deal with, as all 12 leads are provided. To overcome this difficulty, researchers has adopted two different strategies [9]. On the one hand, take as reference for each recording the lead in which their automatic delineation result is closer to manual annotations, thus assuming that only one lead was effectively taken into account to perform manual annotations. On the other hand, take as effective reference the closest automatically delineated point to each manual annotation, regardless of the lead where this takes place. Both strategies are oriented to get an unfair advantage of the database under test because of its full sope annotations.

3.2. Variable annotation criteria

Because of the criteria followed by physicians to locate the fiducial points is unclear, as there exists a lack of consensus in the scientific community about the precise location of the boundaries of a P-wave, generally it is not possible to categorically label an annotation as erroneous or imprecise. However, in some specific cases it is hardly debatable that the annotations are severely defective.

This occur when the annotated point is significantly far from the intuitive area in which an annotation could be considered as well located, as shown in Fig. 1, where common annotations to both channels for two P-waves can be observed. The waves were taken, among many other similar examples found, to exhibit that this is not a particular recording issue. Both leads are displayed because of the aforementioned lack of information about the channel taken into account during the annotation procedure.

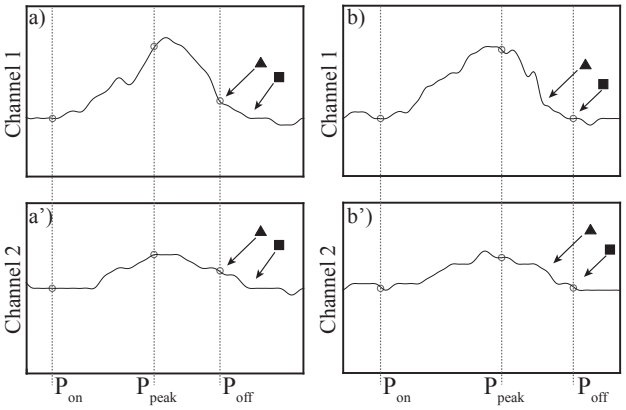

Figure 2. Examples of variable annotation criteria (triangle and square) in two P-waves from recording *sel803* of the QTDB. a) and a') show both channels of the third annotated P-wave, whereas b) and b') show the seventh P-wave. The full scope fiducial points locations are indicated with a dotted line. Remark the dissimilar criteria in a) and b).

Another circumstance in which an annotation can be unequivocally recognized as erroneous, despite the annotation criterion, takes place when the criterion itself varies between two waves of similar morphology. Figure 2 displays an example of two waves collected from the same recording. Observe how how the offset annotation in both waves has been carried out according to different criteria. The two approximate positions according to each annotation criterion are indicated with two different symbols.

3.3. The relevance of noise

Finally, it must be taken into consideration that the signals, and specifically the P-waves because of their generally low amplitude, are deeply affected by noise. Thus, annotating under noisy conditions may render to undesired mistaken fiducial points. Although expert physicians are trained to overcome these adverse conditions and, in many times, they success in ignoring the presence of noise, in other occasions, they may fail despite making similar decisions. This can be easily revealed by a simple denoise process, as the applied in Figure 3, in which a wavelet-based denoising approach has been applied [10]. Two different P-waves are shown, a) and b), with their respective manual annotations that seems to be approximately well located. However, after noise reduction, a different reality is shown for a'), where a late onset has been mistakenly annotated. By contrast, the fiducial points in b') seem to preserve a reasonable location.

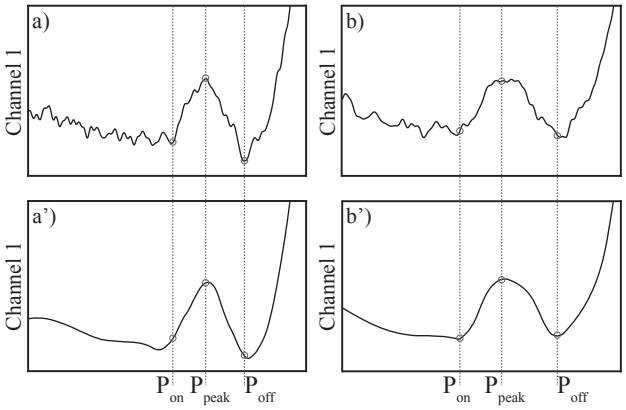

Figure 3. Example of noise effect in annotation reliability for two consecutive P-waves in the first channel of recording *sel230* from the QTDB. a) and b) P-waves of beats 30 and 31. a') and b') Resulting waves and annotations after ECG denoising.

4. Methodology and results

All recordings of the QTDB, to a greater or lesser extent, are affected by noise and consequently also their annotations. To approximately quantify this fact and other issues in the QTDB, an automatic delineator has been applied to P-waves before and after Wavelet-based denoising [10]. Next, the average absolute difference between automatic and manual annotations was computed. Both channels were delineated and the error in each case was computed as the time difference from automatic to the nearest manual annotation.

An adaptive P-wave delineation method, based on fitting P-waves by Gaussian functions, has been applied due to its robustness under noisy recordings [11]. A total of 96 recordings from the QTDB were analyzed, as those with less than three consecutive annotated P-waves were discarded. Results showed that automatic annotations were closer to manual annotations for noisy ECGs and farther in the case of denoised ECGs. An unreal improvement in delineation performance for noisy ECGs was obtained for P-wave onset, peak and offset in 45.83%, 57.29% and 56.25% of the recordings, respectively. Therefore, the influence of noise and (maybe) other aspects leading to mistaken annotations in the QTDB are highly relevant and should be considered seriously.

5. Discussion

As shown in Figures 1 to 3, the existence of inaccurate annotations of P-waves within the QTDB is undeniable, as previous studies have also reported [12]. In fact, other studies have manually reannotated the QTDB before the application of ECG delineation algorithms [13]. Further-

more, defective annotations are not the only source of error for developing automatic delineation methods. Thus, for cases where different criteria are adopted indistinctly, as shown in Figure 2, even if the correctness of both locations could be considered, no automatic delineator could ever meet the two criteria. This situation would involve an error for the algorithm in any case when comparing with the reference of manual annotation. It is, therefore, necessary to define a clear annotation criterion.

Finally, the presence of noise affected considerably the annotations. Thus, any delineator applied to noisy or denoised ECGs will render different fiducial point locations. In fact, delineation under noisy conditions provided better results with respect to manual annotations, but they will be, actually, far from being accurate, thus affecting adversely to outstanding P-wave delineators.

It is difficult to know to what extend these inaccurate annotations have influenced previous results in the literature [9], or even if any of them have could taken advantage of these misplacements. However, what seems to be fairly evident is that this validation method is deficient and its improvement may be presented as the first obstacle to overcome for the development of reliable and clinically useful tools for the delineation of ECG waveforms.

6. Conclusions

In this study, several defects related to the annotations of the QTDB, the generally recognized reference for the validation of ECG delineation algorithms, have been highlighted. There have been identified, among others, the lack of information about the specific lead annotated in each case, the diversity of criteria during the annotation process or the effect of noise in the result of manual annotation. This latter source of error has been demonstrated to have a decisive effect on the outcome of automatic P-wave delineation methods. Thus, to improve the development of reliable and precise delineation methods, as well as to be able to trust on their validation process, one out of two conditions have to be satisfied: either the review of manual annotations on the QTDB, by minimizing all deficiencies highlighted in this study, or the adoption of another alternative more accurately annotated database as a reference.

Acknowledgements

Research supported by grants TEC2014–52250–R and DPI2017–83952–C3 MINECO/AEI/FEDER, UE.

References

[1] Sörnmo L, Laguna P. Ch. 6 - the electrocardiogram-a brief background. In Bioelectrical Signal Processing in Cardiac and Neurological Applications, Biomedical Engineering. Burlington: Academic Press. ISBN 978-0-12-437552-9, 2005; 411 – 452.

[2] Moody GB, Mark RG. The impact of the mit-bih arrhythmia database. IEEE Engineering in Medicine and Biology Magazine May 2001;20(3):45–50. ISSN 0739-5175.

[3] Taddei A, Distante G, Emdin M, Pisani P, Moody GB, Zeelenberg C, Marchesi C. The European ST-T database: standard for evaluating systems for the analysis of ST-T changes in ambulatory electrocardiography. European Heart Journal 1992;13(9):1164–1172.

[4] Willems JL, Arnaud P, Bemmel JHV, Bourdillon PJ, Degani R, Denis B, Graham I, Harms FMA, Macfarlane PW, Mazzocca G, Meyer J, Zywietz C. A reference data base for multilead electrocardiographic computer measurement programs. Journal of the American College of Cardiology 1987;10(6):1313 – 1321. ISSN 0735-1097.

[5] Laguna P, Mark RG, Goldberg A, Moody GB. Database for evaluation of algorithms for measurement of QT and other waveform intervals in the ECG. In Computers in Cardiology. 1997; 673–676.

[6] Magnani JW, Williamson MA, Ellinor PT, Monahan KM, Benjamin EJ. P-wave indices: current status and future directions in epidemiology, clinical, and research applications. Circ Arrh and electroph Feb 2009;2:72–9.

[7] Rieta JJ, Alcaraz R. The Genesis of the Electrocardiogram (ECG). In Wiley Encyclopedia of Electrical and Electronics Engineering. Hoboken, NJ, USA: John Wiley & Sons, Inc., February 2017; 1–15.

[8] Zhang JW, Liu X, Dong J. CCDD: An enhanced standard ECG database with its management and annotation tools. Int Jrnl on Artificial Intelligence Tools 2012;21(05).

[9] Beraza I, Romero I. Comparative study of algorithms for ECG segmentation. Biomedical Signal Processing and Control April 2017;34:166–173.

[10] Bora PK, Sinha R, Yadav SK. Electrocardiogram signal denoising using non-local wavelet transform domain filtering. IET Signal Processing February 2015;9(1):88–96.

[11] González F, Alcaraz R, Rieta JJ. Electrocardiographic P-wave delineation based on adaptive slope gaussian detection. In Computing in Cardiology Conference (CinC), volume 44. IEEE, 2017; In press.

[12] Lenis G, Pilia N, Oesterlein T, Luik A, Schmitt C, Dössel O. P-wave detection and delineation in the ECG based on the phase free stationary wavelet transform and using intracardiac atrial electrograms as reference. Biomedizinische Technik 2016;61(1):37–56.

[13] Martínez A, Alcaraz R, Rieta JJ. Application of the phasor transform for automatic delineation of single-lead ECG fiducial points. Physiol Meas 2010;31(11):1467–1485.

Address for correspondence:

Francisco González Molina
Electronic Engineering Department, Building 7F
Universidad Politécnica de Valencia
Camino de Vera, s/n, 46022, Valencia, Spain
E-mail: fgmolina@upv.es

Método para la Delineación de Ondas P en el ECG Basado en Modelado Gaussiano

F. González Molina[1], R. Alcaraz Martínez[2], J.J. Rieta Ibáñez[1]

[1]BioMIT.org, Dep. de Ingeniería Electrónica, Universitat Politécnica de Valencia, España, {fgmolina, jjrieta}@upv.es
[2]Grupo de Inv. en Electrónica, Telecom. y Bioingeniería, Univ. de Castilla-La Mancha, España, raul.alcaraz@uclm.es

Resumen

El estudio de la onda P en el electrocardiograma es fundamental para caracterizar posibles defectos de conducción que anticipen patologías cardíacas como la fibrilación auricular. Por ello, es necesario el desarrollo de métodos fiables que, de forma automática, detecten y delineen este tipo de ondas. Siguiendo este propósito, en los últimos años se han propuesto muchas estrategias de delineación diferentes. Sin embargo, todas ellas comparten el mismo principio de suavizado agresivo de las ondas para facilitar su delineación, lo cual puede provocar alteraciones morfológicas sustanciales que impliquen una delineación imprecisa. Como alternativa, el método que se presenta en este trabajo opta por un acondicionamiento menos agresivo de la señal y la generación de modelos Gaussianos para cada onda. Así, estos modelos ejercen como asistentes para la delineación de las ondas P, que se realiza mediante la diferenciación de éstas y el establecimiento de un umbral de pendiente adaptativo que tiene en cuenta información sobre el histórico de las ondas previamente delineadas. Este método se validó haciendo uso de los registros de la base datos anotada QT de Physionet. Los resultados de la delineación automática, comparados con las anotaciones, reportaron una sensibilidad del 100 % y un error medio y desviación típica para inicio, pico máximo y final de las ondas P de 4.71±9.59 ms, 2.82±6.69 ms y 0.60±9.79 ms, respectivamente. Estos resultados muestran que la estrategia seguida proporciona una delineación precisa y estable, mejorando otros métodos presentes en la literatura.

1. Introducción

La onda P en el electrocardiograma (ECG), siendo la representación de la actividad eléctrica auricular, se considera la fuente de información no invasiva más fiable sobre la conducción eléctrica en esta región del corazón [1]. Algunas características morfológicas de esta onda, como su duración o dispersión, entre otras, se han asociado con una mayor incidencia y recurrencia de la fibrilación auricular, la arritmia sostenida más frecuente [2]. Sin embargo, la falta de una técnica estándar de medición, así como de un consenso claro acerca de la localización exacta de los límites de estas formas de onda, hacen que delimitar las ondas P sea una tarea compleja. Además, la delineación manual requiere de mucho tiempo y los resultados de la misma pueden variar considerablemente en función de factores diversos como la experiencia del cardiólogo, su grado de cansancio y concentración o la presencia de ruido en la señal [3]. Como respuesta a ello, se han desarrollado una gran variedad de métodos automáticos de delineación de ondas P basados en diferentes estrategias, que van desde el uso de transformadas matemáticas, como la transformada fasorial [4] o la transformada Wavelet [3, 5], hasta la diferenciación de la señal del ECG [6], entre otras. El método que en este estudio se presenta está basado en la diferenciación de la señal, tomando como referencia el propuesto por Laguna et al. [6], pero con diferencias significativas, como son el cálculo de un umbral de pendiente adaptativo teniendo en cuenta las características morfológicas de las anteriores ondas P delineadas o la creación de un modelo Gaussiano para cada onda P que ayude a su delineación. De esta manera, se ha diseñado un algoritmo capaz de detectar y delinear con precisión una amplia variedad de ondas P, siendo más respetuoso con las diferentes morfologías de las ondas y más estable que otros métodos previos.

2. Método

2.1. Preprocesado

Antes de aplicar a la señal de ECG el algoritmo de delineación en sí, ésta debe pasar por un proceso previo de acondicionamiento. En esta etapa, inicialmente, la señal es remuestreada, si no lo estaba ya, a 1 kHz. Seguidamente, la línea base se elimina mediante la substracción de su envolvente y la componente de frecuencia correspondiente al ruido provocado por la red eléctrica se anula mediante filtrado adaptativo. A continuación, el ruido de alta frecuencia procedente de la actividad eléctrica muscular se reduce, aplicando un método basado en la transformada Wavelet y un filtrado bidireccional paso bajo cuya frecuencia de corte se ha establecido en 70 Hz, un valor bastante superior a los tomados por otros métodos comparables [3, 6]. La selección de este filtrado, menos agresivo de lo habitual en otros delineadores, está justificada por la deseable reducción de los transitorios que se produce en la cercanía del complejo QRS y la demostrada existencia, en la onda P, de componentes de frecuencia mayor de los que normalmente se contemplan [7]. Para finalizar el preprocesado de la señal, se realiza una localización supervisada de los picos R a lo largo de ella [8].

2.2. Algoritmo de delineación adaptativo

En el método propuesto, las ondas P a delinear no son tratadas de forma independiente, sino que ciertos parámetros calculados a partir de aquellas anteriormente delineadas son usados para guiar la localización de los puntos fiduciales de cada nueva onda. Entre estos parámetros se incluyen la distancia aproximada entre el pico R correspondiente y la onda P (dPR); la duración aproximada de ésta (durP),

ISBN: 978-84-9082-797-0, pags. 465- 468

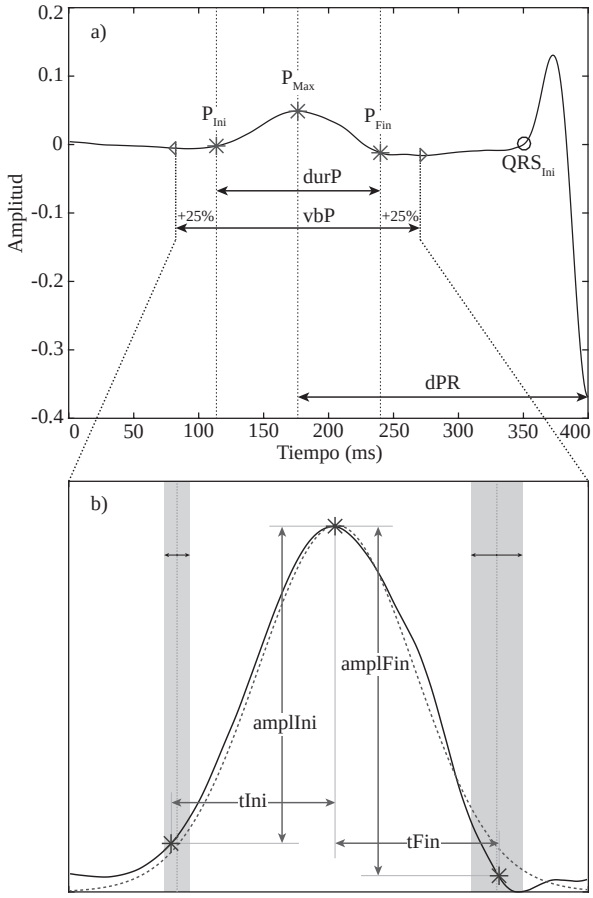

Figura 1. *(a) Señal de referencia sobre la que se muestran, con un círculo, la posición estimada del inicio del complejo QRS (QRS_{Ini}) y, con asteriscos, los puntos fiduciales de la onda P. Además, se exhiben la distancia entre onda P y pico R (dPR) y la duración de la onda P (durP) junto con el de la ventana de búsqueda (vbP), calculada a partir de ella. (b) La misma onda P de (a) expandida (línea continua) y los parámetros morfológicos de la misma. También se muestran, sombreados, los intervalos de búsqueda de las posiciones de inicio y final de onda centrados en los homólogos del modelo Gaussiano (línea discontinua).*

que define una ventana de búsqueda expandiendo su anchura por cada lado un 25 % (vbP); el tipo de morfología; la diferencia en tiempo y amplitud entre pico máximo y cada uno de los límites de onda (amplIni, amplFin, tIni, tFin) y algunos coeficientes iniciales de la función Gaussiana para facilitar la búsqueda del mejor nuevo ajuste. Algunos de estos parámetros se muestran en la Figura 1. Así, estos parámetros se van actualizando con cada nueva onda procesada, con un ratio de impacto de un 20 % sobre el valor existente. Además, antes de ello, se comprueba si la diferencia entre ambos valores es mayor a un 25 %. En tal caso, la onda es catalogada como anormal y no se actualizarán los valores, obteniendo, así, un registro a tiempo real sobre las ondas P cuya morfología se aleja de la norma.

Naturalmente, para dar un valor inicial a estos parámetros, se hace necesaria la inclusión de una etapa de inicialización en la que se crea una onda P de referencia, de la que obtener estos datos. Para ello, se toman los tramos de señal previos a los cinco primeros picos R detectados y, mediante un promediado, se crea un segmento de señal que se llamará, también, de referencia. Sobre este segmento, del que se muestra un ejemplo en la Figura 1.a, se realizarán de forma secuencial los procesos de detección de la onda P, clasificación de su morfología y delineación. Tras ello, tanto la primera como la última etapa se aplican a cada nueva onda P de forma individualizada.

2.3. Detección

Para la detección de la onda P, se ha optado por una búsqueda simple del pico de mayor amplitud en una ventana de búsqueda determinada. Inicialmente, para el caso de la onda P de referencia, la ventana de búsqueda se extiende desde el inicio del complejo QRS previamente estimado, hacia atrás en la señal de referencia, con una duración igual a un tercio de la mediana de las distancias RR. Así, se obtiene un valor inicial para el parámetro dPR, que posteriormente se usará para el cálculo de la posición donde centrar las nuevas ventanas de búsqueda para cada onda P con respecto a su correspondiente onda R.

En torno al pico máximo detectado, se aísla un tramo de señal resultando en la onda P a delinear. La longitud de esta señal, para el caso inicial de referencia, se ha establecido en 180 ms, ampliándose o reduciéndose en 20 ms para casos de intervalo RR promedio demasiado largo (>900 ms) o demasiado corto (<600 ms), respectivamente. Posteriormente, esta longitud se adaptará según la longitud específica de la onda P de referencia, dando valor inicial al parámetro vbP. En la Figura 1.a se muestra de forma visual la prolongación simétrica de durP para la obtención del ancho de la ventana de búsqueda, o vbP.

2.4. Clasificación

Tras detectar la onda P de referencia, ésta debe ser clasificada como monofásica positiva, monofásica negativa o bifásica, ya sea con polaridad positiva-negativa o negativa-positiva. Para este fin se usa un árbol de decisión basado en ajustes Gaussianos que se describe a continuación.

Primero, se genera una función Gaussiana de manera que se ajuste de la mejor forma posible a la onda P de referencia. En caso de que el coeficiente de correlación de Pearson entre la onda y su modelo supere el valor establecido de 0.7, lo que de aquí en adelante se considera un buen ajuste, se clasifica como monofásica positiva y se termina el proceso de clasificación. En caso contrario, se repite la operación con la onda invertida. Si en este nuevo caso sí se obtine un buen ajuste, entonces la onda se clasifica como monofásica negativa y si no, como bifásica. Para este último caso, además, se busca el segundo pico de la onda con polaridad contraria al inicialmente detectado. Por tanto, la onda P de referencia se vuelve a centrar en el punto medio entre ambos picos y se perseguirá un buen ajuste aumentando el orden de la función Gaussiana.

Este proceso inicial de clasificación morfológica de la onda P no se vuelve a repetir en el posterior procesado individualizado de ondas, pues se asume que las ondas P del ECG bajo estudio mantienen un tipo de morfología similar a lo largo del tiempo de registro.

2.5. Delineación

Esta última etapa de delineación es prácticamente igual para el caso de la onda P de referencia que para las ondas individuales. La única diferencia es que, para el caso inicial, únicamente se considera un candidato para cada punto fiducial, mientras que para el resto sí pueden existir varios aspirantes a límite de onda. En este último caso, se elige aquel candidato más cercano a la posición que, con respecto al pico máximo, definan las distancias históricamente calculadas, amplIni y tIni para el inicio de onda y amplFin y tFin para el final.

La delineación comienza con la generación del modelo Gaussiano que mejor se ajuste a la señal correspondiente a la onda P aislada, que en el caso de la de referencia ya se obtuvo en la etapa anterior de clasificación. De esta forma, en primer lugar se produce la diferenciación del modelo Gaussiano, identificando para cada mitad de onda los valores máximos donde la señal presenta los puntos de mayor pendiente. Después, a partir de cada uno de ellos, se calcula un umbral de pendiente que se usa para localizar, en cada caso, los límites de la onda como los primeros puntos en excederlo. Seguidamente, una vez los puntos fiduciales del modelo Gaussiano se han identificado, en torno a sus respectivas posiciones se define un intervalo de búsqueda como los que se muestran en la Figura 1.b en forma de área sombreada. Así, se repite el mismo proceso de diferenciación y búsqueda de puntos donde la pendiente exceda el umbral calculado con la señal real, pero restringiendo la búsqueda al intervalo establecido, cuya anchura depende de lo bien que se ajuste el modelo a la señal real, esto es, siendo más estrecho mientras más parecido sea el ajuste Gaussiano a la onda P real. En la Figura 1.b se puede observar cómo para la posición de inicio de onda este intervalo es más estrecho que para la del final. Ello es debido a que, en este caso, la primera mitad de la onda P se ajusta mejor al modelo Gaussiano.

Para determinar la relación matemática entre los valores de pendiente máxima y la correspondiente pendiente en el límite de onda que definiese el umbral, dos cardiólogos expertos delinearon manualmente un total de 60 ondas P. De esta forma, se llegó a la conclusión de que la función matemática que mejor reflejaba la relación entre pendiente máxima y umbral es la siguiente:

$$Umb(x) = \frac{0.0058 \cdot x}{x + 0.012}, \tag{1}$$

donde x es la pendiente máxima de la onda y Umb el umbral resultante.

Evidentemente, el éxito o no de la delineación depende en gran medida de lo bueno que sea el ajuste Gaussiano. Por ello, a la hora de lidiar con ondas P asimétricas, situación en la que en ningún caso será posible generar un ajuste Gaussiano satisfactorio, se opta por un tratamiento especial. Así, en los casos en los que alguna de las mitades de la onda P no se ajuste bien a su mitad correspondiente del modelo, lo cual se evalúa mediante el ya citado coeficiente de correlación de Pearson, se tomará dicha mitad y se unirá con su propia imagen especular, creando de esta forma una onda P artificial completamente simétrica, de la cual únicamente una mitad tendrá que ser delineada.

Método	P. V.	P_{Ini}	P_{Max}	P_{Fin}
Este método	Se(%)	100	100	100
	$\mu \pm \sigma$(ms)	4.7±9.6	2.8±6.7	0.6±9.8
A. Martínez et al. [4]	Se(%)	98.65	98.65	98.65
	$\mu \pm \sigma$(ms)	2.6±14.5	32±25.7	0.7±14.7
J.P. Martínez et al. [5]	Se(%)	98.87	98.87	98.87
	$\mu \pm \sigma$(ms)	2.0±14.8	3.6±13.2	1.9±12.8
P. Laguna et al. [6]	Se(%)	97.7	97.7	97.7
	$\mu \pm \sigma$(ms)	14±13.3	4.8±10.6	−0.1±12.3

Tabla 1. *Comparación del desempeño de algunos de los métodos de delineación de onda P más relevantes presentes en la literatura mediante los resultados obtenidos por medio de dos Parámetros de Validación (P. V.) haciendo uso de la base de las datos anotada QT.*

3. Evaluación del Método

El desempeño del método de delineación propuesto se evaluó aplicando éste a los registros de la base de datos estándar de referencia QT de Physionet [9]. Esta base de datos contiene 105 registros de 15 minutos de duración de ECGs de dos derivaciones, en cada uno de los cuales, al menos, hay 30 latidos manualmente anotados. Contiene dos grupos de anotaciones realizadas por sendos cardiólogos. Sin embargo, para este estudio, únicamente se tomó como referencia el que contiene un número de anotaciones significativamente mayor. Así, se compararon las distancias en tiempo entre las citadas anotaciones manuales y las propias resultantes del método automático. A partir de la discrepancia en tiempo o error, se ha obtenido un resultado global en términos del valor medio del error (μ) y desviación típica (σ) según propusieron Martínez et al. [5]. También se ha calculado el porcentaje de puntos fiduciales anotados correctamente detectados mediante la sensibilidad (Se %), definida como:

$$\mathrm{Se}(\,\%) = \frac{\mathrm{TP}}{\mathrm{TP} + \mathrm{FN}}, \tag{2}$$

donde TP, verdaderos positivos, corresponde al número de anotaciones correctamente detectadas y FN, falsos negativos, a las no detectadas.

4. Resultados

Los resultados del método, expuestos en la Tabla 1, se obtuvieron tras evaluar la delineación de un total de 3176 ondas P anotadas de 96 de los registros de la base de datos QT. Los registros *sel102*, *sel221*, *sel232*, *sel310*, *sel36*, *sel37*, *sel50* se descartaron al no contar con anotaciones de ondas P con las que comparar las detecciones del método y los registros *sel104* y *sel36*, por no presentar un mínimo de tres ondas P anotadas consecutivas y, por tanto, no poder explotar la naturaleza adaptativa del algoritmo. Además, en la tabla de resultados se presentan los aportados por otros métodos de delineación de onda P relevantes que han hecho uso de la base de datos QT.

5. Discusión

Los buenos resultados obtenidos, mostrados en la Tabla 1, tras haber delineado más de 3000 ondas P procedentes de una gran diversidad de registros específicamente seleccionados para reflejar la variabilidad presente en el mundo real [9], demuestran que el método propuesto es una buena opción para detectar y delinear de manera precisa ondas P, sin importar su morfología. Además, los extraordinarios resultados de desviación típica que se han obtenido, mejorando a los otros delineadores, reflejan que las estrategias seguidas confieren al método una gran estabilidad que refuerza su fiabilidad. Por último, estos valores, tanto para el inicio como para el final de la onda P, se encuentran por debajo de los límites de tolerancia aceptables establecidos por el grupo de trabajo CSE, que son, respectivamente, 10.2 y 12.7 ms [10].

Por otro lado, en la Tabla 1 se observa que los resultados de error medio, aunque bastante buenos, son mejorados en algunos casos por otros métodos. Sin embargo, este parámetro de validación puede ser engañoso, pues podría beneficiarse de la compensación producida entre delineaciones prematuras y tardías. Esta fuente de desconfianza se podría evitar si se tomase el error absoluto como alternativa a este parámetro estándar de validación.

Una de las principales ventajas que presenta el algoritmo presentado con respecto a otros, basados en complejas transformadas matemáticas [3–5], es que se desarrolla íntegramente en el dominio del tiempo. Esta característica permite detectar fácilmente ondas con morfologías anómalas y tener un registro de las mismas, aumentando la información proporcionada y haciendo de éste un método muy versátil. Además, al ser una estrategia más intuitiva y cercana al modo de proceder de los cardiólogos durante la anotación manual de registros, permite que estos puedan guiar o asistir más fácilmente en el desarrollo de posibles futuras mejoras del método.

6. Conclusiones

En este estudio se ha presentado un método novedoso capaz de detectar y delinear automáticamente y de forma precisa cualquier tipo de onda P. Está basado en la diferenciación de la onda y el uso de modelos Gaussianos y de información sobre el histórico de ondas procesadas para asistir la delineación de cada onda P. Todas estas particularidades han permitido alcanzar unos resultados, con respecto a las anotaciones manuales de la base de datos QT, que mejoran a otros métodos presentados en la literatura. Además, el algoritmo diseñado admite nuevas funcionalidades, como la detección de ondas con morfología anómala o la posibilidad de guardar registros sobre la evolución de ciertos parámetros morfológicos de estas ondas a lo largo de la señal. Por tanto, este método se presenta como una solución para la identificación de cambios progresivos en las propiedades de propagación eléctrica auriculares que, eventualmente, pueda ayudar a reconocer procesos internos, como el remodelado auricular, o predecir la ocurrencia de episodios arrítmicos, como la fibrilación auricular.

Agradecimientos

Trabajo financiado por los proyectos TEC2014–52250–R y DPI2017–83952–C3 MINECO/AEI/FEDER, UE.

Referencias

[1] Platonov PG. Atrial conduction and atrial fibrillation: What can we learn from surface ECG? Cardiology Journal 2008; 15(5):402–407.

[2] Magnani JW, Williamson MA, Ellinor PT, Monahan KM, Benjamin EJ. P-wave indices: current status and future directions in epidemiology, clinical, and research applications. Circulation Arrhythmia and electrophysiology Feb 2009;2:72–9.

[3] Lenis G, Pilia N, Oesterlein T, Luik A, Schmitt C, Dössel O. P-wave detection and delineation in the ECG based on the phase free stationary wavelet transform and using intracardiac atrial electrograms as reference. Biomedizinische Technik 2016;61(1):37–56.

[4] Martínez A, Alcaraz R, Rieta JJ. Application of the phasor transform for automatic delineation of single-lead ECG fiducial points. Physiological Measurement 2010; 31(11):1467–1485.

[5] Martínez JP, Almeida R, Olmos S, Rocha AP, Laguna P. A wavelet-based ECG delineator evaluation on standard databases. IEEE Transactions on Biomedical Engineering 2004; 51(4):570–581.

[6] Laguna P, Jané R, Caminal P. Automatic detection of wave boundaries in multilead ECG signals: Validation with the CSE database. Computers and Biomedical Research 1994; 27(1):45–60.

[7] Sörnmo L, Laguna P. Chapter 6 - the electrocardiogram-a brief background. In Bioelectrical Signal Processing in Cardiac and Neurological Applications, Biomedical Engineering. Burlington: Academic Press. ISBN 978-0-12-437552-9, 2005; 411 – 452.

[8] Kohler B, Hennig C, Orglmeister R. The principles of software QRS detection. Engineering in Medicine and Biology Magazine IEEE 2002;21(1):42–57.

[9] Laguna P, Mark RG, Goldberg A, Moody GB. Database for evaluation of algorithms for measurement of QT and other waveform intervals in the ECG. In Computers in Cardiology. 1997; 673–676.

[10] The CSE working party. Recommendations for measurement standards in quantitative electrocardiography. European heart journal Oct 1985;6:815–25.

Estudio Sobre la Fiabilidad de las Anotaciones en la Base de Datos QT de Physionet

F. González Molina[1], R. Alcaraz Martínez[2], J.J. Rieta Ibáñez[1]

[1]BioMIT.org, Dept. de Ingeniería Electrónica, Universitat Politécnica de Valencia, España, {fgmolina, jjrieta}@upv.es
[2]Grupo de Inv. en Electrónica, Telecom. y Bioingeniería, Univ. de Castilla-La Mancha, España, raul.alcaraz@uclm.es

Resumen

La base de datos QT (BDQT) es un referente en análisis electrocardiográfico gracias a dos factores: la amplia variedad de morfologías que contiene y las anotaciones manuales, que determinan los puntos fiduciales de un buen número de latidos. Por ello, es una referencia habitual en la validación de delineadores de ECG. Sin embargo, un porcentaje significativo de sus anotaciones se ha calificado como impreciso, lo cual hace que ningún algoritmo de delineación, por eficiente que sea, pueda conseguir un resultado óptimo. En este trabajo se analizan tanto las imprecisiones de anotación, como la influencia del ruido en el ECG durante la anotación. Se han estudiado las anotaciones en ondas P porque este efecto es mayor para ondas de baja amplitud. Estas anotaciones se compararon con el resultado de aplicar un delineador automático a la señal original con ruido y, después, reduciendo éste mediante un método eficiente basado en la transformada Wavelet. Los resultados mostraron que las anotaciones automáticas se encontraban más cerca de las manuales para el caso de señal ruidosa en un porcentaje significativo de los registros, evidenciando la influencia del ruido en la localización de las anotaciones manuales. Concretamente, esta mejora irreal en la delineación se obtuvo para el inicio, pico máximo y final de onda P, en el 45.83 %, 52.29 % y 56.25 % de los registros, respectivamente. Por tanto, para mejorar la fiabilidad de la validación de delineadores, se hace necesaria la revisión de las anotaciones de la BDQT o el reemplazo de ésta por otra mejor anotada.

1. Introducción

Para poder ser usado en un contexto clínico, cualquier algoritmo de procesado de ECG debe ser validado mediante la evalución de su rendimiento en un contexto lo más realista posible [1]. Para ello, es necesaria la disponibilidad de bases de datos lo suficientemente extensas como para que cubran la gran diversidad de patrones de ondas que los registros de ECG pueden presentar [1]. Además, para el caso específico de métodos como los delineadores de ondas, son necesarias anotaciones que definan de forma precisa los instantes de tiempo en los que ocurren estos eventos. Para poder confiar en las anotaciones, éstas deben haber sido minuciosamente realizadas de forma manual por expertos. Sin embargo, son muchos los factores que pueden influir negativamente en este proceso y, por tanto, comprometer su resultado.

Los investigadores tienen a su disposición un número considerable de bases de datos estándares de ECG, cuyas características propias están estrechamente ligadas al objetivo específico por el cual se crearon inicialmente. Dos de ellas son la base de datos de arritmias MIT-BIH [2] y la base de datos AHA, que se desarrollaron para evaluar el desempeño de distintos detectores de arritmias. Por otro lado, la base de datos europea ST-T se creó como respuesta al creciente interés en el análisis del segmento ST-T como indicativo de isquemia miocárdica [3]. Sin embargo, ninguna de las bases de datos hasta ahora mencionadas contiene anotaciones manuales que definan los límites y el pico máximo de las ondas del ECG, algo fundamental para la validación de algoritmos automáticos de delineación. Así, respondiendo a esta necesidad, surgieron la base de datos de mediciones multiderivación CSE [4] y la base de datos QT (QTDB) [5]. Sin embargo, debido a características distintivas, como la posibilidad de acceso libre o una mayor cantidad de ondas anotadas de forma manual por expertos, esta última base de datos se ha posicionado como la referencia más usada para la validación de delineadores de onda P en los últimos años. No obstante, las anotaciones de la BDQT no son siempre precisas, lo cual puede llegar a generar desconfianza en su uso como vía de validación de algoritmos de procesado de ECG. Por ello, en este estudio se evaluará la calidad de las anotaciones de la BDQT, para el caso de la onda P, y se analizará el origen de los posibles errores en la localización de las mismas.

2. Base de datos QT

La BDQT, disponible gratuitamente en Physionet, está compuesta por un total de 105 registros de ECG de dos canales con una duración de quince minutos cada uno. Estas señales se seleccionaron de otras bases de datos existentes, específicamente, de forma que reflejasen la amplia variabilidad de morfologías que puedan presentar las ondas del ECG en el mundo real [5]. Además, esta base de datos contiene anotaciones manuales que marcan la posición de inicio, pico máximo y final de la onda P; inicio y final del complejo QRS; pico y final de la onda T y, si estuviese presente, pico y final de la onda U. Por cada registro, se proporcionan anotaciones de, al menos, 30 latidos seleccionados para representar el patrón de forma de onda predominante en la señal.

Esta base de datos consta de dos grupos de anotaciones realizadas por sendos expertos. Sin embargo, uno de los conjuntos contiene únicamente 11 registros anotados, por lo que rara vez se ha usado para validar algún método de delineación de ECG. Debido a ello, este estudio se centra en el análisis del grupo con mayor número de anotaciones.

ISBN: 978-84-9082-797-0, pags. 469- 472

El proceso de anotación manual de señales es una tarea lenta y compleja. Además, variables tales como la experiencia del anotador, su grado de concentración y cansancio, la fiabilidad y precisión de la herramienta de anotación usada, o la presencia de morfologías anómalas en la señal, pueden influir en el resultado final de la anotación, comprometiendo su exactitud.

Asimismo, las señales del ECG se ven afectadas en gran medida por diversas fuentes de ruido, como el producido por la actividad eléctrica de los músculos cercanos al corazón, la red eléctrica o un mal contacto del electrodo usado para la obtención de la señal [6]. El problema de estas perturbaciones es que pueden producir alteraciones de la auténtica morfología de la señal. Además, para ondas de baja amplitud, como la onda P, este efecto se acrecienta. Por ello, la onda P se ha seleccionado en el presente trabajo como objeto para la evaluación de las anotaciones manuales de la BDQT. Además, el estudio de esta onda ha despertado un creciente interés debido a la demostrada relación existente entre sus características morfológicas y ciertas afecciones cardíacas, como la recurrencia de la fibrilación auricular [7].

3. Análisis de la fiabilidad de la BDQT

3.1. Anotaciones multiderivación

En el proceso de anotación manual de los registros de la BDQT, se analizaron ambos canales simultáneamente, y la decisión sobre la posición de cada punto fiducial se tomó de forma que ésta fuese común para las dos derivaciones [5]. Sin embargo, es conocido que la disposición en el tiempo de las distintas ondas del ECG es diferente en función de la derivación considerada en cada caso, pues cada una corresponde a una proyección distinta del vector cardíaco [8]. Por tanto, este modo de proceder, unido a la falta de información acerca de cuál de los dos canales se utilizó como referencia de la anotación en cada caso, dificulta el uso de esta base de datos anotada como método de validación de algoritmos de delineación.

Para superar este obstáculo, los desarrolladores de este tipo de algoritmos se han inclinado por dos estrategias diferentes [9]. Por un lado, algunos han optado por asumir que para la anotación de cada registro se consideró únicamente una de las derivaciones, tomando así, como referencia para cada uno de ellos, el canal en el que las correspondientes al método automático se acerquen más a las manuales. Por otro lado, otros desarrolladores han decidido tomar como referencia, para cada punto marcado manualmente en la base de datos, la anotación automática más cercana a él, sin importar a qué derivación corresponda. Ambas estrategias, de un modo u otro, están orientadas a obtener una ventaja injusta de la base de datos, debido a la forma en la que está anotada.

3.2. Criterios de anotación variables

En la comunidad científica no existe un consenso claro acerca de la posición exacta de los límites de la onda P en el ECG. Por ello, al no conocer el criterio seguido por los expertos para localizar los puntos fiduciales en esta onda, generalmente no es posible clasificar una anotación como errónea o imprecisa de forma categórica. Sin embargo, en algunos casos específicos, es difícilmente debatible que las anotaciones son manifiestamente defectuosas.

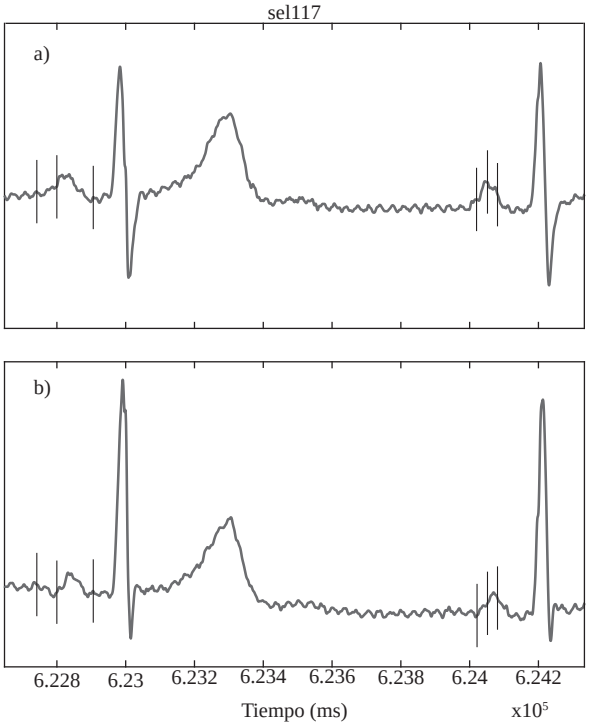

Figura 1. *Ejemplo de los dos canales, a) y b), de un segmento de señal correspondiente al registro sel117 de la BDQT, en los que se muestran, sobre dos ondas P consecutivas, sus discutibles anotaciones manuales mediante líneas verticales. Concretamente, las ondas se corresponden a la 19ª y la 20ª onda P manualmente anotada en este registro. Obsérvense, especialmente, los finales de la segunda onda P en cada registro.*

Uno de los casos en los que esto ocurre es cuando el punto anotado se encuentra significativamente lejos de la zona de la señal en la que una anotación puede ser considerada como correctamente localizada de forma intuitiva. En la Figura 1 se muestra un ejemplo de dos ondas P consecutivas anotadas que responden a esta situación. Se muestran ambos canales debido a la ya comentada falta de información específica acerca de cuál se tomó en cuenta durante el proceso de anotación.

Por otro lado, otra situación en la que el error en la anotación manual es incontestable, tiene lugar cuando se identifican criterios de anotación dispares en ondas cuya morfología es muy similar, tal y como se muestra en la Figura 2. En ella se puede observar cómo el final de dos ondas consecutivasse ha anotado tomando dos criterios dispares, etiquetados como c.1 y c.2. Así, para cada onda, se han marcado tanto la anotación manual original como la posición aproximada que hubiese tenido ésta si para cada caso se hubiese seguido el criterio alternativo. De esta manera, aunque ambos criterios pudieran ser aceptados como válidos, esta manifiesta discordancia evidencia un error en, al menos, una de las anotaciones.

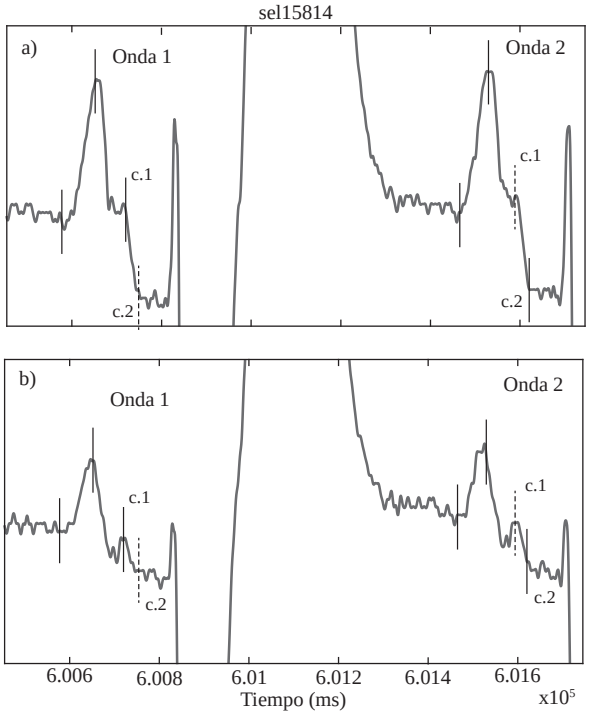

Figura 2. *Ejemplo de los dos canales, a) y b), de un segmento de señal correspondiente al registro sel15814 de la BDQT, en el que se muestra la disparidad de criterios seguidos para la anotación del final de las dos primeras ondas P de este registro. Con líneas continuas se marcan las anotaciones manuales y con discontinuas, la posición aproximada de la anotación si se siguiese el criterio alternativo, c.1 ó c.2., en cada caso*

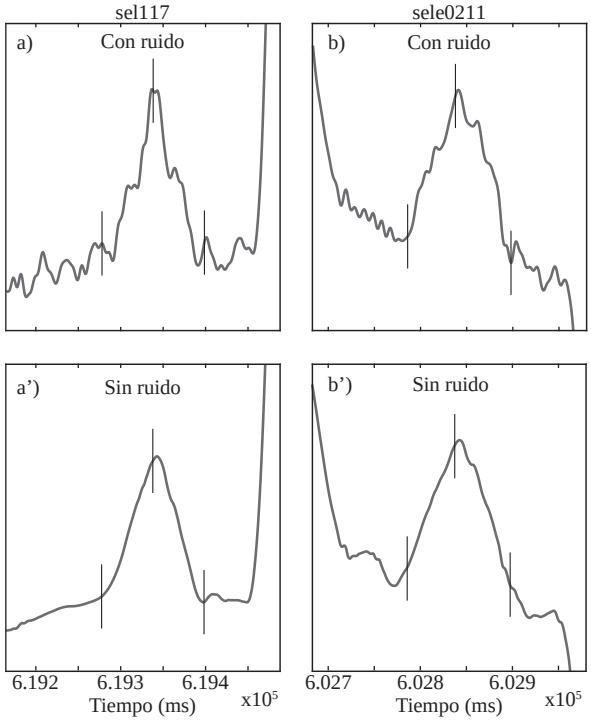

Figura 3. *Ejemplo ilustrativo del efecto del ruido sobre las anotaciones manuales de la BDQT. En a) y b) se muestran, respectivamente, la 16ª onda P anotada del registro sel117 y la 5ª onda del registro sele0211. En a') y b') se presentan las ondas resultantes, junto con sus anotaciones, tras reducir la presencia de ruido en las mismas.*

3.3. Importancia del ruido

Por último, se debe tener en cuenta que las bioseñales como el ECG, y especialmente las ondas P debido a su baja amplitud, se ven profundamente afectadas por ruido. Así, anotar señales que muestren altos niveles de ruido puede provocar desplazamientos indeseados en la posición de los puntos fiduciales marcados. Por ello, aunque los especialistas están entrenados para superar estas condiciones adversas, y muchas veces consiguen obviar la presencia de ruido; otras veces, éste hace que fallen en el proceso de anotación, pese a tomar decisiones similares. Esto puede ser fácilmente revelado por medio de un tratamiento simple de limpieza de ruido de la señal, tal y como se muestra en la Figura 3. En ella se exhiben dos ondas P anotadas, a) y b), y, bajo éstas, en a') y b'), las mismas ondas tras aplicarles un proceso de reducción de ruido basado en la transformada Wavelet [10]. Así, en a) se observan, sobre la señal ruidosa, unas anotaciones que podrían ser consideradas defectuosas, y, tras limpiar la señal, en a') comprobamos que éstas son bastante precisas. Por contra, en b) y b') se presenta el caso opuesto, en el que una onda con ruido pudiera parecer bien anotada y tras reducir la presencia de éste, estas anotaciones pasan a ser más discutibles.

4. Metodología y resultados

Todos los registros de la BDQT, en mayor o menor medida, están afectados por el ruido y, consecuentemente, también sus anotaciones. Para cuantificar aproximadamente este hecho, se ha aplicado un delineador automático a las ondas P, antes y después de reducir la presencia de ruido en la señal mediante un método basado en la transformada Wavelet [10]. Después, para cada caso, se ha calculado el error absoluto medio entre las anotaciones automáticas y las manuales. Esto se ha llevado a cabo aplicando el algoritmo a los dos canales y calculando el error para cada punto fiducial como la diferencia temporal entre la anotación manual y la automática más cercana en cada caso.

Debido a su robustez bajo condiciones de ruido, para la delineación de ondas P se ha aplicado un nuevo método adaptativo basado en la generación de modelos Gaussianos de ondas P [11]. Se analizó un total de 96 registros de la BDQT, descartándose aquellos con menos de tres ondas P consecutivas anotadas.

Los resultados de este estudio mostraron que, en muchos casos, las posiciones de las anotaciones automáticas eran más próximas a las de las manuales para señales de ECG con ruido que sin él. Esta mejora irreal en el desempeño del algoritmo de delineación bajo condiciones de ruido se produjo para el inicio, pico máximo y final de las ondas P en un 45.83 %, 57.29 % y 56.25 % de los registros, respectivamente. Por lo tanto, se ha comprobado que la influencia del ruido y, quizás, otros aspectos que lleven a la incorrecta anotación de las ondas P, son altamente relevantes y deberían ser considerados seriamente.

5. Discusión

Como se ha constatado a lo largo de este estudio, la existencia de anotaciones imprecisas en las ondas P en los registros de la BDQT es un hecho innegable. Ya anteriormente algunos estudios han señalado esta circunstancia, asumiendo el error producido por estos defectos [12]. Asimismo, en otro estudio en el que se introdujo un nuevo delineador de onda P, se reportó una mejora significativa en los resultados obtenidos tras reanotar manualmente los registros de la BDQT [13].

Las anotaciones defectuosas no son la única fuente de error que afecta a la evaluación de los métodos automáticos de delineación. En casos donde se adoptaron criterios de anotación diferentes incluso para ondas de morfología similar, como el mostrado en la Figura 2, es imposible que un algoritmo automático consiga ser preciso siempre. Por ello, estas situaciones implicarán errores, aunque todas las anotaciones pudiesen ser justificadas como correctas.

También se han recalcado los inconvenientes que presenta una referencia anotada mediante una estrategia multiderivación, generando una mayor desconfianza en el resultado que obtenga un método comparado con esta referencia.

Por último, se ha demostrado que la presencia de ruido ha afectado considerablemente al emplazamiento de las anotaciones. Así, el resultado de la localización de los puntos fiduciales para cualquier método automático será distinto en caso de ser aplicado sobre señales con ruido que sin él. De hecho, la delineación automática bajo condiciones de ruido ha proporcionado un mejor resultado, con respecto a las anotaciones manuales de la BDQT, que la misma delineación aplicada sobre los registros limpios de ruido. Esto demuestra que, en muchos casos, un buen delineador capaz de ser completamente inmune al ruido podría verse perjudicado por ello, y otro peor, que acepte erróneamente el ruido como señal real, beneficiado. Es difícil conocer hasta qué punto estas anotaciones desplazadas han podido influir en los delineadores desarrollados en la literatura [9]. Sin embargo, lo que parece ser evidente es que este procedimiento de validación es deficiente, y que su mejora debe ser prioritaria para el desarrollo de métodos de delineación de las ondas del ECG fiables y útiles en la práctica clínica.

6. Conclusiones

En este estudio, se han evidenciado los defectos en las anotaciones manuales de la BDQT, generalmente aceptada para validar delineadores automáticos de ECG. Entre otros, el origen de estos errores es la falta de información sobre el canal específico anotado, la diversidad de criterios durante el proceso de anotación y/o el efecto que la presencia de ruido tuvo en el resultado final de anotación manual de los registros. Este último aspecto se ha cuantificado, demostrando que la relevancia del ruido es significativa y que puede afectar seriamente a los resultados de los diferentes delineadores desarrollados. Por todo ello, para mejorar el desarrollo de delineadores fiables y precisos, así como para poder confiar en su validación, es necesario que las anotaciones manuales de la BDQT sean revisadas y sus registros limpiados de ruido o que se adopte como referencia otra base de datos alternativa. Ésta debería contar con todas las características que se han señalado en este estudio como deseables: Una base de datos de ECGs extensa que presente una gran variedad de morfologías, con anotaciones manuales precisas sobre señales individuales en las que la influencia del ruido sea mínima.

Agradecimientos

Trabajo financiado por los proyectos TEC2014–52250–R y DPI2017–83952–C3 MINECO/AEI/FEDER, UE.

Referencias

[1] Sörnmo L, Laguna P. Ch. 6 - the electrocardiogram-a brief background. In Bioelectrical Signal Processing in Cardiac and Neurological Applications. Academic Press. ISBN 978-0-12-437552-9, 2005; 411 – 452.

[2] Moody GB, Mark RG. The impact of the MIT-BIH arrhythmia database. IEEE Engineering in Medicine and Biology Magazine May 2001;20(3):45–50. ISSN 0739-5175.

[3] Taddei A, Distante G, Emdin M, Pisani P, Moody GB, Zeelenberg C, Marchesi C. The European ST-T database: standard for evaluating systems for the analysis of ST-T changes in ambulatory electrocardiography. European Heart Journal 1992;13(9):1164–1172.

[4] Willems JL, Arnaud P, Bemmel JHV, Bourdillon PJ, Degani R, Denis B, Graham I, et al. A reference data base for multilead electrocardiographic computer measurement programs. Journal of the American College of Cardiology 1987;10(6):1313 – 1321. ISSN 0735-1097.

[5] Laguna P, Mark RG, Goldberg A, Moody GB. Database for evaluation of algorithms for measurement of QT and other waveform intervals in the ECG. In Computers in Cardiology. 1997; 673–676.

[6] Bollmann A, Husser D, Mainardi L, Lombardi F, Langley P, Murray A, Rieta JJ, et al. Analysis of surface electrocardiograms in atrial fibrillation: techniques, research, and clinical applications. Europace Nov 2006;8:911–26.

[7] Magnani JW, Williamson MA, Ellinor PT, Monahan KM, Benjamin EJ. P-wave indices: current status and future directions in epidemiology, clinical, and research applications. Circ Arrh and electroph Feb 2009;2:72–9.

[8] Rieta JJ, Alcaraz R. The Genesis of the Electrocardiogram (ECG). In Wiley Encyclopedia of Electrical and Electronics Engineering. Hoboken, NJ, USA: John Wiley & Sons, Inc., February 2017; 1–15.

[9] Beraza I, Romero I. Comparative study of algorithms for ECG segmentation. Biomedical Signal Processing and Control April 2017;34:166–173.

[10] Bora PK, Sinha R, Yadav SK. Electrocardiogram signal denoising using non-local wavelet transform domain filtering. IET Signal Processing February 2015;9(1):88–96.

[11] González F, Alcaraz R, Rieta JJ. Electrocardiographic P-wave delineation based on adaptive slope gaussian detection. In Computing in Cardiology Conference (CinC), volume 44. IEEE, 2017; In press.

[12] Lenis G, Pilia N, Oesterlein T, Luik A, Schmitt C, Dössel O. P-wave detection and delineation in the ECG based on the phase free stationary wavelet transform and using intracardiac atrial electrograms as reference. Biomedizinische Technik 2016;61(1):37–56.

[13] Martínez A, Alcaraz R, Rieta JJ. Application of the phasor transform for automatic delineation of single-lead ECG fiducial points. Physiol Meas 2010;31(11):1467–1485.